





ARTICLE

# Pluripotent stem cells with low differentiation potential contain incompletely reprogrammed DNA replication

Theodore Paniza<sup>1</sup>, Madhura Deshpande<sup>1\*</sup> , Ning Wang<sup>3\*</sup>, Ryan O'Neil<sup>5</sup>, Michael V. Zuccaro<sup>3,4</sup> , Morgan Elizabeth Smith<sup>3</sup>, Advaita Madireddy<sup>6</sup> , Daylon James<sup>1,2</sup>, Joseph Ecker<sup>5</sup>, Zev Rosenwaks<sup>1</sup>, Dieter Egli<sup>3</sup>, and Jeannine Gerhardt<sup>1,2</sup> 

**Reprogrammed pluripotent stem cells (PSCs) are valuable for research and potentially for cell replacement therapy. However, only a fraction of reprogrammed PSCs are developmentally competent. Genomic stability and accurate DNA synthesis are fundamental for cell development and critical for safety. We analyzed whether defects in DNA replication contribute to genomic instability and the diverse differentiation potentials of reprogrammed PSCs. Using a unique single-molecule approach, we visualized DNA replication in isogenic PSCs generated by different reprogramming approaches, either somatic cell nuclear transfer (NT-hESCs) or with defined factors (iPSCs). In PSCs with lower differentiation potential, DNA replication was incompletely reprogrammed, and genomic instability increased during replicative stress. Reprogramming of DNA replication did not correlate with DNA methylation. Instead, fewer replication origins and a higher frequency of DNA breaks in PSCs with incompletely reprogrammed DNA replication were found. Given the impact of error-free DNA synthesis on the genomic integrity and differentiation proficiency of PSCs, analyzing DNA replication may be a useful quality control tool.**

## Introduction

Reprogrammed patient-specific pluripotent stem cells (PSCs), which can be differentiated into specialized cell types, would be tremendously valuable for regenerative medicine. However, there are subtle differences in the differentiation potential of PSCs. So far, variations in gene expression, mutation rate, or other alterations between PSCs could not fully account for the differences in the differentiation potential among PSCs. Moreover, an increase in genomic instability in reprogrammed PSCs could have a profound impact on their functionality as well as their fate following engraftment, and could increase the risk of cell transformations. One of the most fundamental processes in cells, which ensures genomic stability, is accurate DNA synthesis. Incomplete or incorrect DNA replication induces breaks and mutations in DNA, which could lead to genomic instability. Thus, it is important to assess the accuracy of DNA replication in reprogrammed cells as well as their genomic stability. It is not clear if DNA replication is completely reprogrammed in PSCs and whether the method of reprogramming affects DNA synthesis and the genomic stability.

A decrease in genomic stability during reprogramming can lead to developmental abnormalities (Chia et al., 2017). Therefore, there is a strong rationale to consider DNA replication to be a developmentally relevant factor. Examination of the DNA replication timing has shown that there are regions of the genome that replicate at unique times in specific cell types (Ryba et al., 2011). In mice, the replication timing of some of these DNA regions has been proven to be difficult to reprogram (Hiratani et al., 2010) though cause and consequences were not resolved in this study. Developmentally regulated replication of specific genomic loci has also been identified in human cells (Gerhardt et al., 2016; Schultz et al., 2010). The replication of these loci has to be reprogrammed concurrently with the transcriptional and epigenetic features. Furthermore, early embryos of fast-cleaving organisms and mammalian embryonic stem cells (ESCs), in contrast to differentiated cells, display a high density of DNA replication initiation sites (Ge et al., 2015; Hyrien et al., 1995; Kermi et al., 2017), which seem to be essential for sufficient cell growth in early embryogenesis. It has been reported that the

<sup>1</sup>The Ronald O. Perleman and Claudia Cohen Center for Reproductive Medicine, Weill Cornell Medicine, New York, NY; <sup>2</sup>Department of Obstetrics and Gynecology, Weill Cornell Medicine, New York, NY; <sup>3</sup>Department of Pediatrics, Columbia University, New York, NY; <sup>4</sup>Department of Physiology and Cellular Biophysics, Columbia University Vagelos College of Physicians and Surgeons, New York, NY; <sup>5</sup>Plant Molecular and Cellular Biology Laboratory, Salk Institute, La Jolla, CA; <sup>6</sup>Department of Pediatric Hematology/Oncology, Rutgers University, New Brunswick, NJ.

\*M. Deshpande and N. Wang contributed equally to this paper; Correspondence to Jeannine Gerhardt: [jeg2039@med.cornell.edu](mailto:jeg2039@med.cornell.edu).

© 2020 Paniza et al. This article is distributed under the terms of an Attribution–Noncommercial–Share Alike–No Mirror Sites license for the first six months after the publication date (see <http://www.rupress.org/terms/>). After six months it is available under a Creative Commons License (Attribution–Noncommercial–Share Alike 4.0 International license, as described at <https://creativecommons.org/licenses/by-nc-sa/4.0/>).

high density of replication origins is the result of checkpoint inefficiency in early cell development (Desmarais et al., 2012; Kappas et al., 2000; van der Laan et al., 2013). It has also been shown in humans that hESCs fail to activate Chk1 (Desmarais et al., 2012) and contain a higher amount of dormant origins to protect cells against genomic instability (Ge et al., 2015).

There are several approaches to cell reprogramming. One approach that holds great promise for regenerative medicine is the use of isogenic PSCs (Takahashi et al., 2007; Takahashi and Yamanaka, 2006), from which all kinds of cell types in adult tissues can be generated. Although iPSCs have been extensively evaluated and compared with hESCs, questions remain as to how similar iPSCs are to hESCs, and what risks the iPSCs hold for genomic instability. Numerous large-scale studies have revealed subtle differences between the epigenetics and gene expression profiles of iPSCs and hESCs (Bock et al., 2011; Chin et al., 2009; Deng et al., 2009; Doi et al., 2009; Guenther et al., 2010; Lister et al., 2011; Newman and Cooper, 2010; Nishino et al., 2011), although only a few, if any, genes showed consistent differences. However, it is still not known how the reprogramming process affects DNA synthesis and long-term genomic stability in iPSCs. Furthermore, epigenetic and gene expression analysis alone are not sufficiently predictive or comprehensive in terms of quality control and in identifying stem cell lines that are suitable for therapeutic applications.

Another cell reprogramming approach is a process known as somatic cell nuclear transfer (SCNT; Tachibana et al., 2013; Yamada et al., 2014). PSCs derived by SCNT (NT-ESCs) have been shown to have therapeutic potential. For example, NT-hESCs generated from human donor cells with diabetes 1 phenotype were shown to secrete insulin (Sui et al., 2018; Yamada et al., 2014). SCNT recapitulates developmental events that occur upon normal fertilization, allowing the epigenomic state of the somatic nucleus to be reset to an early embryonic stage. In contrast, iPSCs are generated via the ectopic expression of a key set of embryonic transcription factors. One study showed that in mice, iPSCs retained an epigenetic memory of the source cells, whereas the NT-ESCs did not (Kim et al., 2010). However, in human cells, DNA methylation patterns and gene expression patterns were very similar between NT-hESCs and human iPSCs (Johannesson et al., 2014). Nevertheless, these iPSCs displayed variations in their potential to differentiate into pancreatic  $\beta$  cells (Sui et al., 2018). So far, these differences could not be explained by alterations in cell processes, such as mutation rate or variations in DNA methylation. For stem cell research and therapy, the functionality and genomic stability of stem cells are among the highest priorities. Therefore, the accurate DNA synthesis may play an important role in the ability of cells to proliferate and differentiate in specific cell types.

To determine the DNA replication, we used a single-molecule analysis of replicated DNA (SMARD; Gerhardt et al., 2014a, 2014b). In PSCs reprogrammed by nuclear transfer or with defined factors, we found that DNA replication was incompletely reprogrammed; in particular, fewer DNA replication origins were activated in PSCs with a lower differentiation potential. The decrease in origin activation could lead to incomplete DNA synthesis and result in genomic instability. Indeed, we also

found a higher frequency of DNA breaks in PSCs with a low differentiation potential. Furthermore, our results show that replication in NT-hESCs as well as in iPSCs generated from neonatal cells with a higher differentiation potential was more efficiently reprogrammed than that in iPSCs generated from adult cells. In addition, the reprogramming of DNA replication in PSCs was not influenced by DNA methylation. Thus, our results suggest that an in-depth analysis of DNA replication fidelity in reprogrammed cells might be essential not only as an indicator for the differentiation potential of PSCs but also for the safety of patients who may undergo transplantation using reprogrammed PSCs.

## Results

### Differences in genomic stability and differentiation potential among reprogrammed PSCs

A fundamental concern about stem cells and their differentiated derivatives is their ability to restore physiological functionality and to resist neoplastic transformation in response to endogenous genotoxic stress (Wyles et al., 2014). Variations in differentiation potential were recently observed among isogenic PSCs generated by different reprogramming approaches (Fig. 1, A and B; Sui et al., 2018). In particular, a lower differentiation potential was detected among iPSCs (Fig. 1 B). However, isogenic iPSCs and NT-ESCs showed similar genome-wide gene expression and DNA methylation profiles, as well as comparable numbers of de novo coding mutations (Fig. 1 C; Johannesson et al., 2014). Thus, it is still not clear what causes the differences in the differentiation potential among reprogrammed PSCs. Because cell cycle progression is linked to cell differentiation, we first examined the cell cycle (Fig. S1 A) and did not detect alterations in the cell cycle progression among these isogenic iPSCs and NT-ESCs (Fig. 1 D).

Next, since no obvious differences in gene expression and epigenetics were found, we decided to test whether the variations in the differentiation potential could be explained by an increase in chromosomal instability due to challenges during the DNA replication. Thus, we quantified the micronuclei formation under replicative stress (Fig. 1, E and F). Micronuclei are formed more often when there is an increase in DNA breaks within the cell. DNA breaks can occur as a result of replication defects, which are usually rectified by the DNA repair process. We examined the micronuclei formations in isogenic NT-hESCs and iPSCs, which showed different differentiation potentials. We compared the amount of micronuclei in these cells to the amount of micronuclei in the genetically identical fibroblast line (adult fibroblasts: 1018 and neonatal fibroblasts: BJ) from which they were generated. We calculated the number of micronuclei in cells before and after aphidicolin treatment. Aphidicolin is a polymerase inhibitor that is used to induce replicative stress. We observed a slight increase in micronuclei formation in hESCs, NT-hESCs, and neonatal iPSCs after treatment with aphidicolin. However, more micronuclei were detected in iPSCs generated from adult fibroblasts (adult iPSCs), which showed the lowest differentiation potential (Fig. 1, E and F). The percentage of micronuclei was increased by threefold after aphidicolin

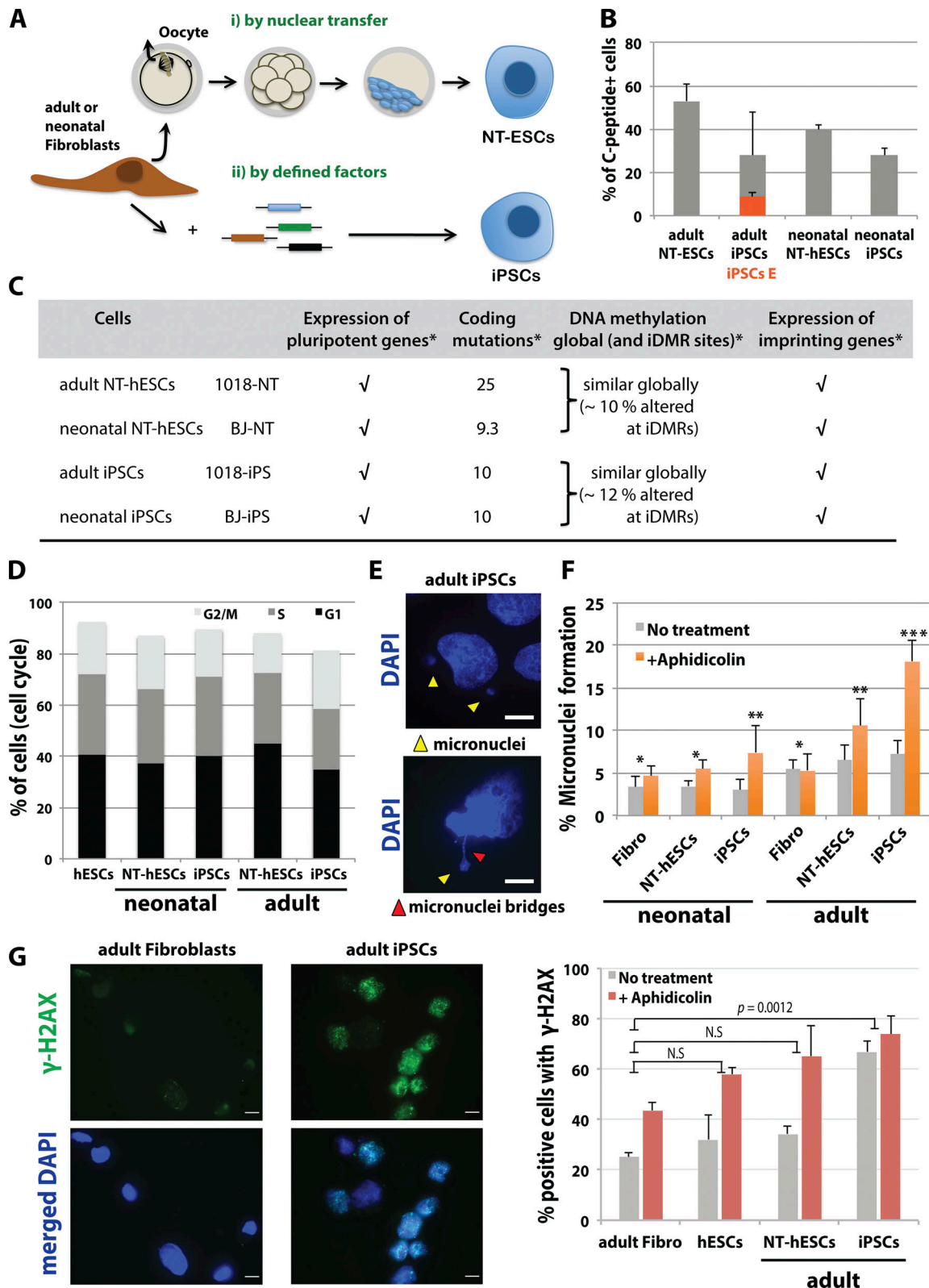


Figure 1. **Characteristics and analysis of the genomic integrity of isogenic PSCs.** (A) Schematic of the steps for cell reprogramming using nuclear transfer (resulting in NT-hESCs) or defined factor (resulting in iPSCs) from neonatal fibroblasts or adult fibroblasts. Both cell lines are isogenic because cells were derived from the same cell source (fibroblasts). (B) Differentiation potential of isogenic NT-hESCs and iPSCs derived from adult (1018) or neonatal (BJ) fibroblasts into C peptide–positive  $\beta$  cells, which is a cell type found in pancreatic islets. The differentiation potential of the adult iPSCs E cell line, which had the lowest differentiation potential (Sui et al., 2018), is shown in orange. (C) Table summarizes the gene expression of pluripotent and imprinting genes, number of coding mutations, and the percentage of altered DNA methylation at imprinted DMRs (iDMRs) and globally in isogenic reprogrammed PSCs (\*data obtained

from [Johannesson et al., 2014](#)). **(D)** Cell cycle analysis (G1, S, and G2/M phase) of isogenic NT-hESCs and iPSCs derived from adult or neonatal fibroblasts. **(E)** Micronuclei and micronuclei bridges were observed in adult iPSCs (DAPI staining; scale bar, 10  $\mu$ M). **(F)** The relative percentage of micronuclei was calculated for each cell line (fibroblasts [Fibro], NT-hESCs, and iPSCs) with and without 0.6  $\mu$ M aphidicolin treatment. Standard deviation is indicated. All results were performed in triplicate, and  $\geq 120$  cells were scored for each experiment (total  $n \geq 360$ ). Standard deviation and P values are indicated in the diagram (\*, NS; \*\*,  $P \geq 0.05$ ; \*\*\*,  $P = 0.001$ ). **(G)**  $\gamma$ H2AX analysis of isogenic NT-hESCs and iPSCs derived from adult (1018) or neonatal (Bj) fibroblasts with and without 0.6  $\mu$ M aphidicolin treatment. Left: Sample picture of  $\gamma$ H2AX- (green) and DAPI- (blue) stained cells (scale bar, 10  $\mu$ M). Right: Quantification of the percentage of  $\gamma$ H2AX-positive cells. Standard deviation and P values are indicated in the diagram. The experiments were repeated three times (total  $n \geq 300$ ).

treatment compared with the fibroblasts line. We also noticed the presence of micronuclei bridges in iPSCs (Fig. 1 E). Although a low rate of micronuclei formation is intrinsic to PSCs, an increase in amount of micronuclei formation is an indication of chromosomal instability. Next, to determine whether there is an increase in genomic instability, we quantified the  $\gamma$ H2AX-positive cells. An increase in the amount of  $\gamma$ H2AX signal in cells is a marker for DNA breaks (Fig. 1 G). We found a similar amount of  $\gamma$ H2AX staining in NT-hESCs and hESCs. With aphidicolin, genomic instability was increased in these cells, as expected. In adult iPSCs, we detected a higher amount of  $\gamma$ H2AX-positive cells with and without aphidicolin than in hESCs and in isogenic NT-hESCs. These results indicated a higher frequency of genomic instability in adult iPSCs.

#### DNA replication is reprogrammed after human SCNT

Error-free duplication of the human genome is crucial to prevent genomic instability and mutations, which could lead to cell transformation or cell death ([Aguilera and Gómez-González, 2008](#); [Bandura and Calvi, 2002](#); [Blow and Gillespie, 2008](#); [Branzei and Foiani, 2010](#)). Because we detected an increase in genomic instability, particularly after the induction of replicative stress, we next analyzed whether defects in the DNA replication could be present in these cells. Since no major differences in the replication timing were found previously among human PSCs ([Ryba et al., 2010](#)), we decided to analyze the DNA replication using a high-resolution single-molecule technique called SMARD (Fig. 2 A; and Fig. S1, B and C). Using SMARD, alterations in the DNA replication program can be visualized, which could be missed using bulk DNA studies. The progression of DNA replication was determined at specific genomic loci, where distinctive DNA replication fork profiles and differences were detected during cell development (Fig. S1 B; [Gerhardt et al., 2016](#); [Schultz et al., 2010](#)). These specific developmentally regulated genomic loci, such as the *Frataxin* (*FXN*) and *Nanog* gene loci, show a different replication profile in hESCs in contrast to differentiated cells ([Gerhardt et al., 2016](#); [Schultz et al., 2010](#)).

First, we determined the replication in PSCs generated by SCNT at these loci (Fig. 2). NT-hESCs were made by replacing of a human oocyte nucleus with a somatic cell nucleus, followed by parthenogenesis (Fig. 1 A). As previously shown, in contrast to differentiated cells, we found active replication initiation sites within the *FXN* locus in 22% of the DNA molecules in unaffected control hESCs (Fig. 2 B; and Fig. S2, A and B; [Gerhardt et al., 2016](#)). In addition, the replication forks progressed in 3'-5' and 5'-3' directions through the *FXN* locus at normal speeds without fork stalling (Fig. 5, D and E). As previously observed in differentiated cells, we found only very few replication origins (7%

of total DNA molecules) in the neonatal fibroblast line from which the neonatal NT-hESCs were derived (Fig. 2 C; [Gerhardt et al., 2016](#)). However, we found that the isogenic neonatal NT-hESCs and a second NT-hESC line (derived from adult fibroblast line 1018) had a similar DNA replication pattern at the *FXN* locus as hESCs (~23% of the DNA molecules contained active replication origins; Fig. 2, D and E). These results show that DNA replication in PSCs reprogrammed by SCNT was comparable to the replication seen in hESCs.

#### DNA replication is incompletely reprogrammed in iPSCs derived from adult cells

Next, we analyzed the DNA replications in iPSCs, which were generated from fibroblasts by the nonviral mRNA reprogramming technology (adult iPSCs E) or by retroviral transduction of the transcription factors Oct3/4, Sox2, Klf-4, and c-Myc in the presence of sodium butyrate ([Ku et al., 2010](#); adult iPSCs B). The adult iPSCs E showed the lowest differentiation potential (Fig. 1 B) and is a line isogenic to adult NT-hESCs, as shown in Fig. 2 E. We found that in contrast to PSCs generated by SCNT, DNA replication in iPSCs differed from hESCs at the *FXN* locus (Fig. 3, A and B). SMARD results showed that very few replication initiation sites were activated at the *FXN* locus in these two iPSCs (4.3% or 7.4% of total DNA molecules, respectively) similar to our previous results ([Gerhardt et al., 2016](#)). Replication with few replication initiation sites in these two iPSCs resembled the replication seen in differentiated cells (Fig. 2 C; [Gerhardt et al., 2016](#)). In contrast, we found more active replication origins at the *FXN* locus in iPSCs derived from neonatal fibroblasts (27% of DNA molecules; Fig. 3 C) than in adult iPSCs. This cell line is isogenic to the neonatal NT-hESCs (Fig. 2 D, generated from the same neonatal fibroblast line, Fig. 2 C). Neonatal iPSCs and NT-hESCs had a higher differentiation potential than that of adult iPSCs (Fig. 1 B). We confirmed these results in a second neonatal iPSC line (21% of DNA molecules contained origins, Fig. S2 D). Thus, our results show that the reprogramming of DNA replication at the *FXN* locus in iPSCs, generated from adult fibroblasts using integrating and nonintegrating methods, was incomplete (Fig. 3 D and Fig. S2 C). Our results also show that the reprogramming of DNA replication is more efficient in iPSCs generated from neonatal cells.

We next analyzed DNA replication in hESCs and iPSCs at a second developmentally regulated gene locus containing the *Nanog* gene (Fig. 3, A-C). Differences in replication fork direction between hESCs and differentiated cells were observed at this locus ([Schultz et al., 2010](#)). Similar to the *FXN* gene locus, we found that the replication at the *Nanog* locus is altered in adult iPSCs compared with hESCs. More replication forks progressed in the 3'-5' direction through the *Nanog* gene locus in iPSCs,

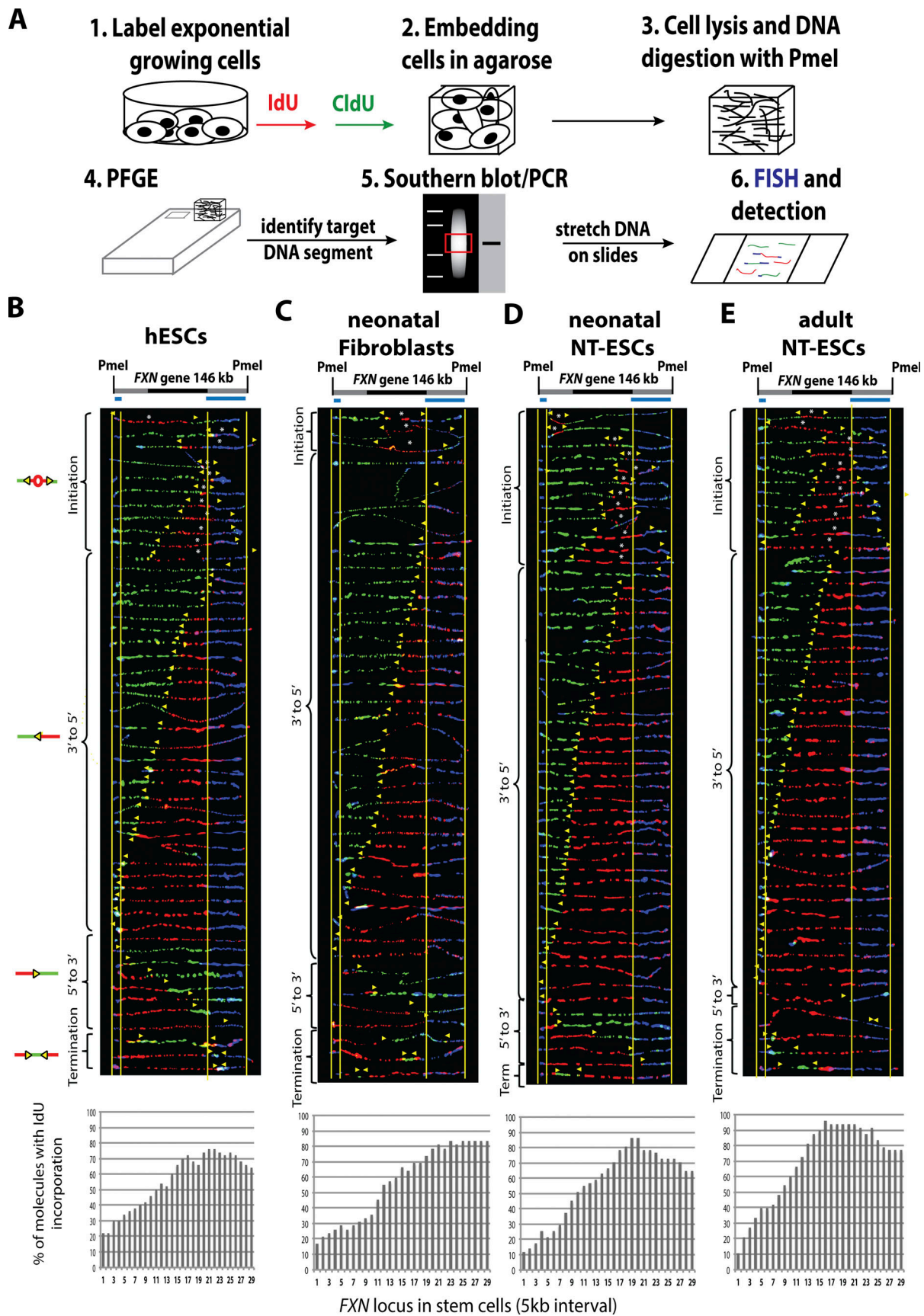


Figure 2. **DNA replication in NT-hESCs is very similar to that in hESCs.** (A) Schematic of the steps of SMARD that enable the visualization of single replicating DNA molecules. First, cells are pulsed with IdU (red) and CldU (green). Cells are then embedded in agarose and lysed. After digestion with *PmeI*

enzyme DNA molecules are separated by PFGE. The DNA segment containing the *FXN* locus is then identified, excised from the gel, and stretched on silanized glass slides. The labeled DNA molecules are detected by immunostaining (red and green) and two FISH probes surrounding the endogenous genomic locus. **(B–E)** Top: Map of the Pmel segment containing the *FXN* gene (black) analyzed with SMARD. The positions of the FISH probes are marked in blue. Middle: Photomicrographs of labeled DNA molecules from hESCs, neonatal fibroblasts, NT-hESCs derived from neonatal (neo NT-hESCs), and adult cells (NT-hESCs) are ordered according to replication fork (yellow arrows) progression in the 5'-3' and 3'-5' directions, replication initiation; and termination. Bottom: The percentage of molecules with IdU incorporation (first pulse) in PSCs is calculated from the DNA molecules shown above.

similar to the replication program seen in differentiated cells (Fig. S3, B and C; Schultz et al., 2010). However, in isogenic NT-hESCs, the replication fork progressed equally in both directions through the *Nanog* locus, as in hESCs (Fig. S3, B and C).

In summary, our results show that the reprogramming of DNA replication was incomplete in human iPSCs in contrast to PSCs generated by SCNT (NT-hESCs). However, iPSCs reprogrammed from neonatal cells have a similar DNA replication program as hESCs, in contrast to the iPSCs reprogrammed from adult cells. These observations suggest that neonatal cells are more efficiently reprogrammed than adult cells. Moreover, incompletely reprogrammed DNA replication would explain the variability in the differentiation potential among these PSCs.

#### The reprogramming of the DNA replication at developmentally regulated and at abnormally methylated loci is not primarily determined by DNA methylation

To identify the cause of incompletely reprogrammed replication in iPSCs, we examined whether aberrant DNA methylation influences the DNA replication in iPSCs. Refined gene expression profiles have revealed small sets of differentially expressed genes and differentially methylated regions (DMRs) in genetic matching sets of hESCs and iPSCs (Liang and Zhang, 2013). To test whether the reprogramming of the DNA replication is influenced by the abnormal CpG methylation in reprogrammed iPSCs, we examined replication at the aberrant methylated *TCERGIL* gene locus (Fig. 4 A). The *TCERGIL* gene locus has been shown to have differential gene expression and differential DNA methylation (Choi et al., 2015). The *TCERGIL* promoter is methylated in the iPSCs but not in hESCs and NT-hESCs (Fig. 4 B). Using SMARD, we found that the replication fork direction, initiation, and termination at the *TCERGIL* gene locus in iPSCs (Fig. 4, D and F) did not differ significantly from the replication observed at the *TCERGIL* gene locus in hESCs and NT-hESCs (Fig. 4, C, E, and F). We detected a similar replication pattern at the *TCERGIL* locus in iPSCs and NT-hESCs despite differential methylation at this locus. The replication forks progressed from both directions through the locus, and only a few replication initiation and termination sites were detected in all cell lines. To summarize, no major alterations were detected in the DNA replication at the abnormally methylated *TCERGIL* gene locus in PSCs, suggesting that aberrant DNA methylation does not alter the replication fork progression and replication initiation at this genomic site.

Next, we determined whether differences in replication at the *FXN* and *Nanog* gene loci could be explained by differential DNA methylation. Thus, we examined DNA methylation at the *FXN* and *Nanog* loci as well. We did not find any differences in the DNA methylation pattern between PSCs at these genomic

loci (Fig. 3 E and Fig. S3 D), indicating that DNA methylation is not the cause of incompletely reprogrammed DNA replication in adult iPSCs.

#### A lower number of replication initiation sites was detected in incompletely reprogrammed iPSCs

Our results show that the reprogramming of the DNA replication at the developmentally regulated *FXN* and *Nanog* loci in iPSCs, generated from adult cells, was incomplete. In particular, fewer active DNA replication origins were detected (Fig. 3 D). Because there were fewer replication initiation sites at the *FXN* gene locus, we wanted to determine whether the number of active replication initiation sites is lower throughout the whole genome in reprogrammed iPSCs. For this purpose, we pulse-labeled cells with IdU and CldU, and then we stretched the genomic DNA on glass slides. Then we analyzed the replication initiation events in three hESCs, four iPSCs (three adult and one neonatal), two NT-hESCs, and two differentiated cell lines using fluorescence microscopy (for examples, see Fig. 5 A, right). We found that ~16% of DNA molecules contained DNA replication origins in hESCs (Fig. 5 A, left), whereas only ~8% of DNA molecules with origins were observed in adult iPSCs. We also found that the percentage of active replication origins in differentiated cells was lower compared with that in hESCs and similar to that in adult iPSCs (~7.8%). In contrast, NT-hESCs, neonatal NT-hESCs, and neonatal iPSCs contained a similar number of replication initiation sites as hESCs (around 16% of molecules). These results agree with the observation that during embryogenesis, more DNA replication origins are used than differentiated cells (Ge et al., 2015; Hyrien et al., 1995; Kermit et al., 2017). It has also been proposed that the use of more dormant replication origins helps to protect hESCs against replicative stress (Ge et al., 2015). Our results show that the genome-wide pattern of DNA replication varies significantly between PSCs and hESCs, and specifically that the frequency of replication initiation is lower in iPSCs generated from adult cells.

It has been reported that in early embryonic development, DNA replication is more rapid and a higher density of origins has been observed than in later developmental stages (Hyrien et al., 1995; Kermit et al., 2017). In addition, it has been shown that the speed of replication forks and DNA synthesis does not slow down after DNA damage in early embryonic cells as it does in adult cells (Kermit et al., 2017). A loosening of the replication checkpoint and a greater number of active replication initiation sites might be needed in ESCs to ensure the completion of DNA synthesis for the rapid cell growth during early embryonic development. The replication checkpoint slows down replication by inhibiting origin firing and reducing the rate of replication

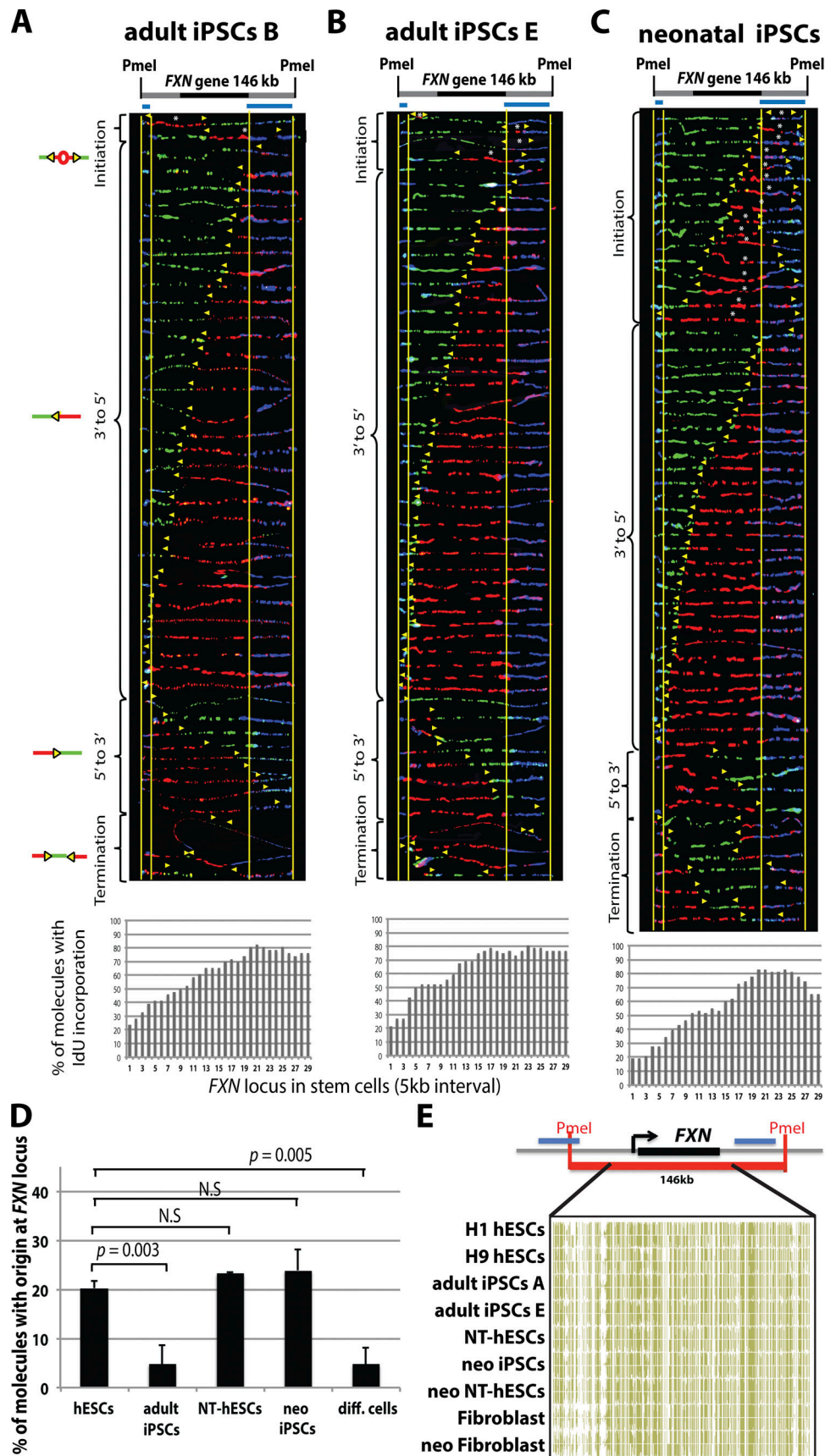


Figure 3. **The DNA replication is altered at the developmentally regulated *FXN* gene locus in iPSCs.** (A–C) Top: Map of the PmeI segment containing the *FXN* gene (marked in black). The positions of the FISH probes are marked in blue, and the DNA segment (146 kb) was analyzed using SMARD. Middle:

Photomicrographs of labeled DNA molecules from hESCs, iPSCs, and NT-hESCs are ordered according to replication fork (yellow arrows) progression in the 5'-3' and 3'-5' directions, replication initiation; and termination. Bottom: The percentage of molecules with IdU incorporation (first pulse) in hESCs, iPSCs, and NT-hESCs is calculated from the DNA molecules shown above. **(D)** Diagram of the percentage of DNA molecules with replication initiation sites from three hESCs (Fig. 2 B, H9 and H14; Gerhardt et al., 2016), three iPSCs (iPSCs B and E, Fig. 3, A and B; and iPSCs NP, Gerhardt et al., 2016), two NT-hESCs (NT-hESCs, Fig. 2 D; and neonatal NT-hESCs, Fig. 2 E), two neonatal iPSCs (see Fig. 3 C and Fig. S2 D), and two diff. cells (neonatal fibroblasts, Fig. 2 C; and diff. H9 cells, Gerhardt et al., 2016). Standard deviation and P values are indicated in the diagram. **(E)** CpG methylation analysis of the *FXN* gene locus using bisulfite sequencing.

fork progression (Ge and Blow, 2010). It has been shown in *Xenopus* and *Drosophila* model systems that the feedback control that slows down the cell cycle during early embryogenesis is not very efficient, and there is no temporal regulation of origins firing orchestrated by the replication checkpoint. Thus, an inefficient replication checkpoint, which likely causes the higher density of replication origins in ESCs, has been detected in early embryos of fast-cleaving organisms and in mammalian ESCs including hESCs (Desmarais et al., 2012; Kappas et al., 2000; van der Laan et al., 2013).

To further examine the cause of the relatively low rate of replication initiation in adult iPSCs, we examined the activity of the replication stress response in reprogrammed PSCs by measuring replication fork speed, fork stalling, and dormant origin activation (Fig. 5, B–G). At the site of DNA damage and fork stalling, the checkpoint activates dormant origins to help ensure the completion of DNA synthesis after fork stalling. As a control, we examined in parallel the efficiencies of the replication stress response in hESCs. In hESCs and NT-hESCs with and without aphidicolin treatment, we detected a similar replication pattern and amount of origins (Fig. 5, A–C). In addition, aphidicolin-treated hESCs and NT-hESCs had only a slightly lower replication fork speed (Fig. 5 D) and no significant replication pause sites (Fig. 5, E and G). Together with the observation that hESCs poorly activate Chk1 (Desmarais et al., 2012), these results suggest a less active replication stress response in hESCs. In contrast, the replication fork speed slowed down significantly and replication forks stalled in adult iPSCs after aphidicolin treatment (Fig. 5, D and F; and Fig. S4). In response to fork stalling, dormant origins were activated at the *FXN* locus and in the genome in adult iPSCs (Fig. 5, A–C). These results together with our previous observation of dormant origins activation and fork stalling after aphidicolin treatment in another iPSCs line (Gerhardt et al., 2016) suggest that iPSCs reprogrammed from adult cells have an altered stress response to aphidicolin compared with hESCs. This would explain the lower number of active replication origins in adult iPSCs, thus providing a mechanistic explanation for the incomplete reprogramming of the DNA synthesis.

## Discussion

Today, cells derived from PSCs are advancing toward clinical application. For example, midbrain dopaminergic neurons derived from iPSCs (Barker et al., 2017) might be applicable as cell replacement therapy for patients with neurodegenerative disorders such as Parkinson's disease (Studer, 2017), macular degeneration (Mandai et al., 2017), and diabetes (Maehr et al., 2009). Some of these applications involve the use of reprogrammed

iPSCs as a source. Here we describe, for the first time, that the reprogramming of DNA replication can be incomplete in reprogrammed human iPSCs. Altered DNA replication and increased chromosomal instability can inhibit cell proliferation and differentiation, and increase the risk of diseases, including cancer (Aguilera and Gómez-González, 2008; Bandura and Calvi, 2002; Blow and Gillespie, 2008; Brnzei and Foiani, 2010; Chia et al., 2017). Proper duplication and segregation of undamaged genetic material to daughter cells are essential for the survival and differential potential to different cell lineages. Because of the impact of DNA replication on genome stability and cell function, assessing reprogrammed stem cells for clinical application may require DNA replication analysis using assays as we have described here.

To exclude genetic background as a possible cause for differences in DNA replication (Choi et al., 2015), we compared isogenic reprogrammed NT-hESCs and iPSCs that were generated from the same human somatic cells (Johannesson et al., 2014). In addition, besides the reprogramming technique, the cell source may exert an influence on the efficiency of cellular reprogramming. It has been shown that adult fibroblasts are less amenable to reprogramming than fetal and neonatal fibroblasts (Park et al., 2008a,b; Rajarajan et al., 2012). When pluripotency was induced with defined factors, fetal and neonatal cells formed iPSC colonies faster and yielded greater numbers of cells compared with adult cells (Hansel et al., 2014; Park et al., 2008a,b; Rajarajan et al., 2012). Furthermore, the generation of an all-iPSCs mice from adult cells is exceedingly inefficient, whereas it is possible to generate such mice from embryonic fibroblasts (Boland et al., 2009). Thus, we analyzed the DNA replication in iPSCs and NT-hESCs reprogrammed from adult and neonatal cells. SMARD revealed that the replication pattern in NT-hESCs and neonatal iPSCs was very similar to that in hESCs. In contrast, isogenic iPSCs had an altered DNA replication program. Thus, comparing the DNA replication patterns among hESCs, NT-hESCs, and iPSCs derived from neonatal or adult cells provided us with a better understanding of the efficiencies of different reprogramming approaches.

## Cause of incomplete reprogrammed DNA replication

Studies by our laboratory and other groups have shown that the replication fork progression at certain specific genomic loci is cell type-specific and regulated during cell development such as at the *FXN* locus (Aladjem, 2007; Gerhardt et al., 2016; Ryba et al., 2011; Schultz et al., 2010). To better understand the reprogramming of DNA replication in iPSCs, we examined the *FXN* and *Nanog* loci, where the DNA replication is developmentally regulated in human cells (Gerhardt et al., 2016). Previously we found that aberrant replication and replication fork stalling at



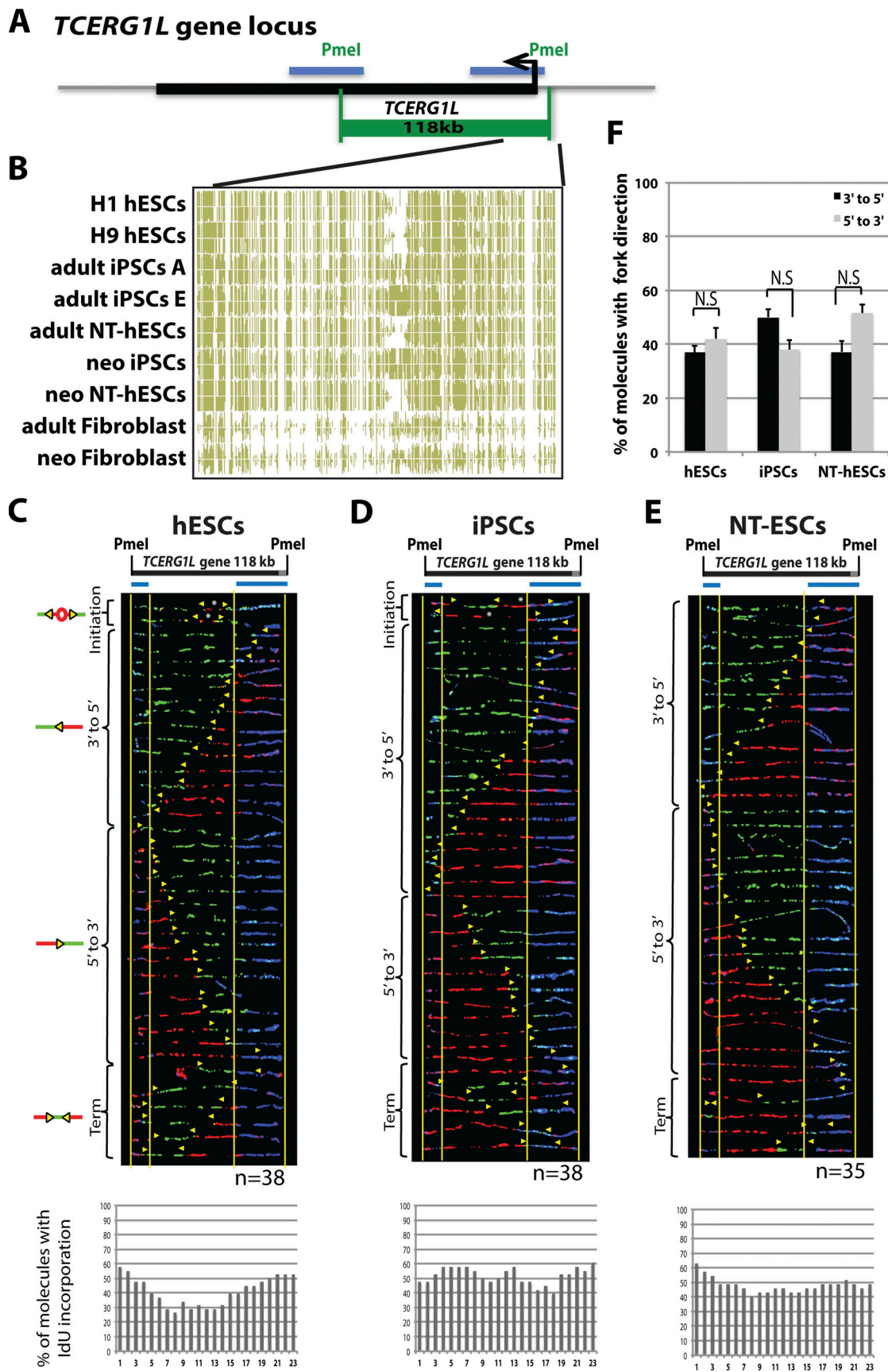


Figure 4. DNA replication is similar at the differentially methylated *TCERG1L* regions in iPSCs and hESCs. (A) Map of the *TCERG1L* locus containing the positions of the FISH probes, which are marked in blue, and the DNA segment (118 kb) analyzed using SMARD (green). (B) CpG methylation analysis of the

*TCERG1L* gene locus using bisulfite sequencing. **(C–E)** Top: Map of the *TCERG1L* segment with FISH probes. Middle: Photomicrographs of labeled DNA molecules from hESCs, iPSCs, and NT-hESCs are ordered according to replication fork (yellow arrows) progression in the 5′-3′ and 3′-5′ directions; replication initiation; and termination. Bottom: The percentage of molecules with IdU incorporation (first pulse) in hESCs, iPSCs, and NT-hESCs is calculated from the DNA molecules shown above. **(F)** Diagram of the percentage of DNA molecules with replication fork progression in the 3′-5′ and 5′-3′ directions in hESCs, iPSCs, and NT-hESCs. Standard deviation and P values are indicated in the diagram (P values: hESCs = 0.19, iPSCs = 0.068, NT-hESCs = 0.065).

the *FXN* locus led to genomic instability in stem cells derived from Friedreich’s ataxia patients (Gerhardt et al., 2016). Our data showed incomplete reprogramming of the replication in these two genomic regions in reprogrammed iPSCs, in particular a decrease in origin activation. Although replication timing has been linked previously to DNA methylation, our results surprisingly show that alterations in the replication program seems not to be primarily determined by the DNA methylation at the developmental regulated loci that were examined.

In addition, it was previously reported that ESCs contain a higher density of origins than differentiated cells, which was suggested to be important for sufficient cell growth and genomic stability at this early developmental stage. Our data suggest that the low number of replication origins in iPSCs derived from adult cells is the result of an altered response to aphidicolin. This could impede the completion of DNA synthesis in these cells and cause genomic instability (Fig. S5). Indeed, we found a larger increase in micronuclei formation and DNA breaks in iPSCs after the induction of replicative stress.

#### Importance of completely reprogrammed DNA replication

The replication program is cell type-specific (Gerhardt et al., 2016; Ryba et al., 2011; Schultz et al., 2010), and it has been shown that analysis of the replication timing can be used to identify specific cell types (Ryba et al., 2011). Our results suggest that alterations in DNA replication program could affect the cell integrity and the cell differentiation potential of PSCs. If the replication is not reprogrammed completely to the pluripotent state, PSCs might only be able to differentiate to certain cell types. This means that reprogrammed PSCs with incompletely reprogrammed DNA synthesis might only differentiate to cell types from which they were derived. In addition, reduced replication initiation in specific regions of the genome could delay the DNA replication at these sites and cause DNA breaks and mutations. Delayed DNA replication could also interfere with chromatin organization as well as with the transcription of specific genes (Brambati et al., 2015). Altered replication fork progression could increase the frequency of collisions between replication and transcription machinery at genes essential for cell type-specific differentiation. For example, we found altered replication at the developmentally regulated *FXN* gene locus, which was reported to be important for cell differentiation into neuroectoderm cells (Santos et al., 2001). It has been shown also that Frataxin deficiency in mouse pancreatic islets causes a decrease number of proliferating  $\beta$  cells and diabetes in older mice due to elevated reactive oxygen species and increased frequency of apoptosis (Ristow et al., 2003). This might explain the lower differentiation potential of adult iPSCs into pancreatic  $\beta$  cells.

Our data point to NT-hESCs as a type of reprogrammed cells with a more completely reprogrammed DNA replication and

DNA methylation. Neonatal NT-hESCs and somatic NT-hESCs both had DNA replication profiles similar to that of hESCs. While generation of PSCs by SCNT selects for the ability of a cell to advance through embryonic developmental steps, the induction of pluripotency by defined factors selects for growth in the pluripotent state, not for developmental competence. Those differences in the reprogramming process could explain the different functional outcomes. Notably, NT-hESCs produce viable mice (Wakayama et al., 2013) more consistently than iPSCs (Wakayama et al., 2013).

Nevertheless, reprogramming by SCNT requires oocytes from donors, which might limit the scalability of reprogramming using that technique. Thus, it is also important to find a reliable approach for generating iPSCs using defined factors that will result in complete reprogramming. We found differences in the reprogramming efficiency of the DNA replication depending on the somatic cell source, as fetal and neonatal progenitor cells also seem to yield greater amounts of reprogrammed cells than adult progenitor cells (Hansel et al., 2014; Park et al., 2008a,b; Rajarajan et al., 2012). Our data show that DNA replication in reprogrammed neonatal iPSCs is similar to that in hESCs, suggesting that the reprogramming of DNA synthesis and the differentiation potential are more complete in iPSCs generated from neonatal cells than in adult cells. Thus, reprogramming PSCs from neonatal cells would be a good alternative approach. Neonatal cells obtained from umbilical cord blood have also become increasingly available in recent years and could be an accessible cell source for regenerative medicine. In addition, since adult iPSCs show less differentiation ability in general than NT-hESCs and neonatal iPSCs (Sui et al., 2018), replication defects and an increase in genomic instability could explain the differences in the differentiation potential of PSCs. A more completely reprogrammed DNA replication process could also explain the higher efficiency in derivation of PSCs from neonatal cells. In summary, reprogrammed cells with accurate replication and without replication defects would be beneficial for research and regenerative medicine due to their lower risk of genomic instability. Future studies should focus on genome-wide identification of loci that can serve as markers of complete replication reprogramming, including a comparison of iPSCs with hESCs replication timing profiles (Ding et al., 2020). The study presented here provides the rationale for evaluating DNA replication in reprogrammed PSCs as a routine quality control step before potential clinical use.

## Materials and methods

### Cell culture

All experiments with human cells were reviewed and approved by the Columbia and Weill Cornell Institutional Review Board

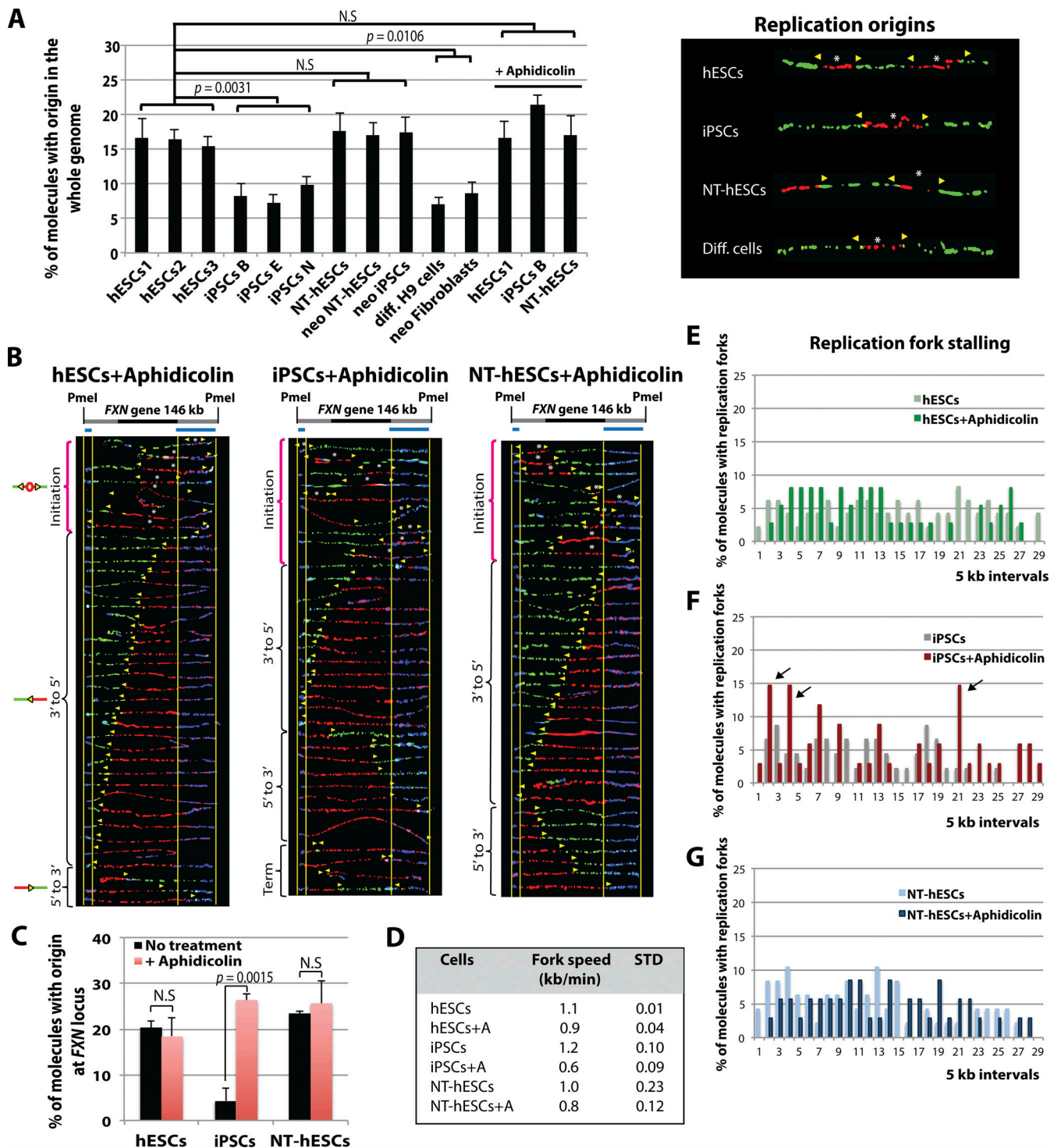


**Figure 5. iPSCs show a decrease in DNA replication initiation and altered response to aphidicolin compared with hESCs.** (A) Left: Diagram of the percentage of DNA molecules with replication initiation sites in unaffected hESCs, iPSCs, NT-hESCs, neonatal iPSCs, and differentiated cells (isogenic fibroblasts line BJ and H9 rosettes), as well as aphidicolin-treated hESCs, iPSCs, and NT-hESCs. Standard deviation and P values are indicated in the diagram ( $n \geq 100$ ). Right: Examples of DNA fibers containing replication origins from which the percentage of molecules with origins is calculated (see left) are shown for each cell line: hESCs, iPSCs, NT-hESCs, and differentiated cells. (B) SMARD; Top: Map of the Pmel segment containing the *FXN* gene. Middle: Photomicrographs of labeled DNA molecules from hESCs, iPSCs, and NT-hESCs treated with 0.4  $\mu$ M aphidicolin are ordered according to replication fork (yellow arrows) progression in the 5'-3' and 3'-5' directions, replication initiation, and termination sites. (C) Diagram of the percentage of DNA molecules with replication initiation sites at the *FXN* locus in hESCs, iPSCs, and NT-hESCs treated with aphidicolin (calculated from the replication pattern shown in B and without aphidicolin (from Fig. 2, B and E; and Fig. 3 A)). (D) Replication fork speed with aphidicolin (A) was calculated from the replication pattern shown in B as well as without aphidicolin from the replication pattern shown in Fig. 2, B and E; and Fig. 3 A in hESCs, NT-hESCs, and iPSCs. Fork speed calculation is described in the Materials and methods section. STD, standard deviation. (E-G) The percentage of molecules with replication forks for each 5-kb DNA interval was calculated at the *FXN* locus in hESCs (green, E), iPSCs (red, F) and NT-hESCs (blue, G) treated with (calculated from the replication pattern shown in B) and without aphidicolin (from Fig. 2, B and E; and Fig. 3 A). Black arrows point at stalled replication forks.

(IRB), including hESCs (H1, H9, H14, WCMC4), NT-hESCs (1018-NT-ES), neonatal NT-hESCs (Johannesson et al., 2014), human iPSCs (iPSCs B: 8399; iPSC E: 1018-iPS-E; iPSCs A: 1018-iPS-A, iPSCs N: NP), neo iPSCs (BJ-iPS-O, BJ-iPS-M; Johannesson et al., 2014), neonatal fibroblasts (BJ), fibroblasts (1018) and neural stem cells (diff. H9 cells; Gerhardt et al., 2016; Johannesson et al., 2014). Human pluripotent stem cell lines were cultured on Geltrex-coated plates in StemFlex Medium (A3349401; Gibco) to 90% confluence and passaged with TrypLE (12605036; Life Technologies). The medium for culturing fibroblast cells contains DMEM (10569; Gibco) supplemented with 10% FBS (S11150; Atlanta Biologicals), 1% GlutaMAX (35050-061; Gibco), 1% NEAA (11140-050; Gibco), 0.1 mM 2-Mercaptoethanol (21985; Gibco), and 1% penicillin/streptomycin (400-109; Gemini). hESCs were cultured on Matrigel (Corning) in medium (containing 80% Knockout Dulbecco's modified Eagle's medium, 20% knockout serum replacement supplemented with 2 mM L-glutamine, 1% nonessential amino acids, 100 U/ml penicillin, 100 µg/ml streptomycin, 0.1 mM β-mercaptoethanol and 4 ng/ml fibroblast growth factor 2, all from Gibco). For production of conditioned medium, mouse embryonic fibroblasts were plated at 1 million cells/cm<sup>2</sup> in DMEM with 10% FBS overnight. The next day, this medium was replaced with HESC medium overnight for conditioning. The next day, the medium was removed, and 10 ng/ml FGF2 was added to conditioned medium before use. For treatment with aphidicolin, cells were incubated with 0.4 µM aphidicolin at 37°C for 16 hrs. After the treatment, the cells were harvested using Trypsin (Gibco). For the SMARD experiment, cells were dissociated into single cells using tryptase (Gibco, 10 min) and ~10<sup>7</sup> cells were grown in the presence of the nucleosides.

### Cell cycle analysis

To perform EdU (5-ethynyl-2'-deoxyuridine) staining, we used the Click-iT<sup>TM</sup> EdU Alexa Fluor 488 Imaging Kit (C10337; Invitrogen) according to the manufacturer's instructions. The cells were cultured for 1 h in EdU. Next for nuclear staining, the samples were washed with cold PBS and centrifuged (5 min, 1,000 rpm) at 4°C. RNase was added to a final concentration of 0.2 µg/µl, and incubated at room temperature (RT) for 30 min. Then, 1 ml of 2 µg/ml Hoechst 33342 was added to the samples, which were incubated at RT for 30 min. After washing, each sample was analyzed using the BioRad ZE5 at the Columbia University Stem Cell Initiative Flow Cytometry Core.

### SMARD

The cells were grown at 37°C for 4 h in the presence of 25 µM 5-iodo-2'-deoxyuridine (Sigma-Aldrich). After washing cells with PBS, hESCs medium with 25 µM 5-chloro-2'-deoxyuridine (Sigma-Aldrich) was added to the cultures, and the cells were incubated for an additional 4 h. The cells were lifted with Accutase or Trypsin. Following centrifugation, the cells were re-suspended at 3 × 10<sup>7</sup> cells per ml in PBS. Melted 1% InCert agarose (Lonza Rockland, Inc.) in PBS was added to an equal volume of cells at 42°C. The cell suspension was pipetted into a chilled plastic mold with 0.5 by 0.2-cm wells with a depth of 0.9 cm for preparing DNA gel plugs. The gel plugs were allowed

to solidify on ice for 30 min. Cells were lysed in buffer containing 1% *n*-lauroylsarcosine (Sigma-Aldrich), 0.5 M EDTA, and 20 mg/ml proteinase K. The gel plugs remained at 50°C for 64 h and were treated with 20 mg/ml proteinase K (Roche Diagnostics), every 24 h. Gel plugs were then rinsed several times with Tris-EDTA (TE) and once with phenylmethanesulfonyl fluoride (Sigma-Aldrich). The plugs were washed with 10 mM MgCl<sub>2</sub> and 10 mM Tris-HCl (pH 8.0).

The genomic DNA in the gel plugs was digested with 40 units of *PmeI* (New England BioLabs Inc.) at 37°C overnight. The digested gel plugs were rinsed with TE and cast into a 0.7% Sea-Plaque GTG agarose gel (Lonza Rockland, Inc.). A gel lambda ladder PFG marker and yeast chromosome PFG marker (both from New England BioLabs, Inc.) were cast next to the gel plugs. Gel slices from the appropriate positions in the pulsed-field electrophoresis gel (PFGE) were cut and melted at 72°C for 20 min. GELase enzyme (Epicentre Biotechnologies 1 unit per 50 µl of agarose suspension) was carefully added to digest the agarose and incubated at 45°C for a minimum of 2 h. The resulting DNA solutions were stretched on 3-aminopropyltriethoxysilane (Sigma-Aldrich)-coated glass slides. The DNA was pipetted along one side of a coverslip that had been placed on top of a silane-treated glass slide and allowed to enter by capillary action. The DNA was denatured with sodium hydroxide in ethanol and then fixed with glutaraldehyde.

The slides were hybridized overnight with a biotinylated probe (the blue bars diagrammed on the maps indicate the positions of the probes used). The following day, the slides were rinsed in 2× SSC (1× SSC is 0.15 M NaCl plus 0.015 M sodium citrate) 1% SDS and washed in 40% formamide solution containing 2 × SSC at 45°C for 5 min and rinsed in 2 × SSC-0.1% IGEPAL CA-630. Following several detergent rinses (four times in 4× SSC-0.1% IGEPAL CA-630), the slides were blocked with 1% BSA for at least 20 min and treated with Avidin Alexa Fluor 350 (Invitrogen Molecular Probes) for 20 min. The slides were rinsed with PBS containing 0.03% IGEPAL CA-630, treated with biotinylated anti-avidin D (Vector Laboratories) for 20 min, and rinsed again. The slides were then treated with Avidin Alexa Fluor 350 for 20 min and rinsed again, as in the previous step. The slides were incubated with the IdU antibody, a mouse anti-bromodeoxyuridine (Becton Dickinson Immunocytometry Systems), the antibody specific for CldU, a monoclonal rat anti-bromodeoxyuridine (anti-BrdU; Accurate Chemical and Scientific Corporation) and biotinylated anti-avidin D for 1 h. This was followed by incubation with Avidin Alexa Fluor 350 and secondary antibodies, Alexa Fluor 568 goat anti-mouse IgG (H+L; Invitrogen Molecular Probes), and Alexa Fluor 488 goat anti-rat IgG (H+L; Invitrogen Molecular Probes) for 1 h. After a final PBS/CA-630 rinse, the coverslips were mounted with ProLong gold antifade reagent (Invitrogen). A fluorescent microscope (Axioscop 2 M2 with Plan Apochromat 63×/1.4 NA oil differential interference contrast objective; Carl Zeiss) with a camera (CoolSNAP HQ; Photometrics) and IPLab 4.0.8 software (BD) was used to detect the nucleoside incorporation into the DNA molecules. Images were processed with Photoshop CS5 software. Image processing involves alignment of the DNA molecules according to the FISH probes, adjusting of the contrast, and

removing unspecific background signal. Total number of DNA molecules for each cell line were captured from three blinded experiments. The molecules presented are the complete dataset. We used Student's *t* test with two-tailed distribution for P value calculation.

Replication fork speed at the *FXN* locus was calculated using the following equation: Average kb /min = [Length of segment (kb) / Td (min)] / Average number of replication forks for this segment (Norio and Schildkraut, 2001). Td; duplication time of the fragment; the time required for the segment to duplicate (min), which is calculated by the following equation:  $Td = Tp1 \times NRG / (NR + NRG)$  or  $Td = Tp1 \times NRG / (NG + NRG)$ . Tp1 = Time for the first or second labeling (4 hours). NR or NG = the number of molecules fully stained in red or green. NRG = the number of molecules fully stained in both red and green in the segment.

### DNA fiber analysis

To analyze origin density, cells were pulsed labeled with 25  $\mu$ M 5-iodo-2'-deoxyuridine (Sigma-Aldrich) and with 25  $\mu$ M 5-chloro-2'-deoxyuridine (Sigma-Aldrich). The DNA was stretched on glass slides and the incorporated nucleotides were detected by IdU antibody (mouse anti-bromodeoxyuridine, Becton Dickinson Immunocytometry Systems) and CldU antibody (monoclonal rat anti-bromodeoxyuridine [anti-BrdU], Accurate Chemical and Scientific Corporation) as described above. We used Student's *t* test with two-tailed distribution for P value calculation.

### DNA methylation analysis

DNA extraction was performed using the Qiagen DNeasy Blood and Tissue kit (69506). One microgram of genomic DNA was spiked with 5 ng/ $\mu$ l of unmethylated cl857 Sam7 Lambda DNA (D1501; Promega) to later compute non-conversion rate. The DNA was fragmented to 150–200 bp using a Covaris S2 and ligated with mC adapters provided by Illumina. The adaptor-ligated DNA underwent a sodium bisulphite conversion using the MethylCode kit from Life Technologies and then PCR. The samples were sequenced on Illumina HiSeq 2500. The methylation reads were mapped to hg19, and methylation sites called using methylpy (Schultz et al., 2015). The non-conversion rate was computed from each sample by analyzing the cytosine mischaracterization rate on the lambda DNA sequence. Experiments were performed blind.

### Micronuclei assay

For the micronuclei assay, cells were dissociated into single cells using trypsin (Gibco, 10 min). The cells were harvested and resuspended in PBS-EDTA (1 mM EDTA). The cell count was adjusted to 1 million cells/ml, and cells were harvested (~50–100  $\mu$ l / slide) by centrifugation on positively charged slides (VWR) using CytoSpin 4 (Thermo Scientific). The centrifugation was done at 500 rpm for 5 min. The slides were air dried and mounted with Antifade Mountant with DAPI (Invitrogen). The slides were allowed to dry before scoring for micronuclei. The slides were read on Zeiss fluorescence microscopes at 100X magnification. The nuclei were assessed for the presence of micronuclei, and micronuclei bridges. All results were performed in

triplicates, and  $\geq 120$  cells were scored for each experiment. We used Student's *t* test with two-tailed distribution for P value calculation.

### $\gamma$ H2AX detection

Cells were gently placed on polysine-coated slides (Shandon; catalog no. 6776216; lot no. 112216-9). The cells were allowed to settle for 20 min at RT. Liquide was removed by gently tilting the slide and the cells were fixed-permeabilized in PMTEF buffer for 20 min at RT (4% paraformaldehyde, 200 mM PIPES, pH 6.8, 200 mM MgCl<sub>2</sub>, 10 mM EGTA, 0.2% Triton X-100). After fixation-permeabilization, slides were washed three times with PBS. Immunostaining was performed using the primary rabbit monoclonal anti- $\gamma$ -H2AX antibody (9718T; Cell Signaling Technology) and the secondary goat anti-rabbit Alexa-488-conjugated IgG (44125; Cell Signaling Technology). Nuclei were stained with DAPI. We performed three independent blinded experiments. Fluorescence microscopy was used to visually and record cells with positive foci ( $n \geq 150$ ). We used Student's *t* test with two-tailed distribution for P value calculation.

### Online supplemental material

Fig. S1 shows cell cycle analysis and DNA segments analyzed by SMARD, related to Figs. 1, 2, 3, 4, and 5. Fig. S2 shows that the DNA replication program is not altered at the *FXN* in a second neonatal iPSC line and at the *TCERGIL* gene locus, related to Figs. 2, 3, and 4. Fig. S3 shows that DNA replication is altered at the developmentally regulated *Nanog* gene locus in iPSCs compared with hESCs, related to Fig. 2. Fig. S4 shows a table with the percentage of replication forks at the *FXN* locus per each 5-kb segment in adult iPSCs compared with hESCs, related to Fig. 5. In Fig. S5, a model is shown summarizing the results and replication defects in PSCs that could lead to genomic instability and altered cell differentiation potential, related to Figs. 1, 2, 3, 4, and 5.

### Acknowledgments

We thank Alexandra MacWade for proofreading the manuscript.

This work was funded by the Perelman research recruitment gift (J. Gerhardt) and NYSTEM IDEA Award (C32564GG to D. Egli). The studies at the *FXN* locus in iPSCs were supported by National Institutes of Health grant R03 NS106216 (J. Gerhardt).

The authors declare no competing financial interests.

Author contributions: J. Gerhardt and D. Egli conceived and designed the study. M. Smith, D. James, and N. Wang grew PSCs. J. Gerhardt, T. Paniza, and M. Deshpande performed SMARD and  $\gamma$ H2AX experiments and analyzed the results. N. Wang and M.V. Zuccaro performed cell cycle analysis. R. O'Neil and J. Ecker performed the DNA methylation analysis. J. Gerhardt wrote the manuscript. D. Egli, Z. Rosenwaks, and A. Madireddy edited and/or discussed the manuscript.

Submitted: 30 September 2019

Revised: 26 February 2020

Accepted: 13 May 2020

## References

- Aguilera, A., and B. Gómez-González. 2008. Genome instability: a mechanistic view of its causes and consequences. *Nat. Rev. Genet.* 9:204–217. <https://doi.org/10.1038/nrg2268>
- Aladjem, M.I.. 2007. Replication in context: dynamic regulation of DNA replication patterns in metazoans. *Nat. Rev. Genet.* 8:588–600. <https://doi.org/10.1038/nrg2143>
- Bandura, J.L., and B.R. Calvi. 2002. Duplication of the genome in normal and cancer cell cycles. *Cancer Biol. Ther.* 1:8–13. <https://doi.org/10.4161/cbt.1.1.31>
- Barker, R.A., M. Parmar, L. Studer, and J. Takahashi. 2017. Human Trials of Stem Cell-Derived Dopamine Neurons for Parkinson's Disease: Dawn of a New Era. *Cell Stem Cell.* 21:569–573. <https://doi.org/10.1016/j.stem.2017.09.014>
- Blow, J.J., and P.J. Gillespie. 2008. Replication licensing and cancer—a fatal entanglement? *Nat. Rev. Cancer.* 8:799–806. <https://doi.org/10.1038/nrc2500>
- Bock, C., E. Kiskinis, G. Verstappen, H. Gu, G. Boulting, Z.D. Smith, M. Ziller, G.F. Croft, M.W. Amoroso, D.H. Oakley, et al. 2011. Reference Maps of human ES and iPSC cell variation enable high-throughput characterization of pluripotent cell lines. *Cell.* 144:439–452. <https://doi.org/10.1016/j.cell.2010.12.032>
- Boland, M.J., J.L. Hazen, K.L. Nazor, A.R. Rodriguez, W. Gifford, G. Martin, S. Kupriyanov, and K.K. Baldwin. 2009. Adult mice generated from induced pluripotent stem cells. *Nature.* 461:91–94. <https://doi.org/10.1038/nature08310>
- Brambati, A., A. Colosio, L. Zardoni, L. Galanti, and G. Liberi. 2015. Replication and transcription on a collision course: eukaryotic regulation mechanisms and implications for DNA stability. *Front. Genet.* 6:166. <https://doi.org/10.3389/fgene.2015.00166>
- Branzei, D., and M. Foiani. 2010. Maintaining genome stability at the replication fork. *Nat. Rev. Mol. Cell Biol.* 11:208–219. <https://doi.org/10.1038/nrm2852>
- Chia, G., J. Agudo, N. Treff, M.V. Sauer, D. Billing, B.D. Brown, R. Baer, and D. Egli. 2017. Genomic instability during reprogramming by nuclear transfer is DNA replication dependent. *Nat. Cell Biol.* 19:282–291. <https://doi.org/10.1038/ncb3485>
- Chin, M.H., M.J. Mason, W. Xie, S. Volinia, M. Singer, C. Peterson, G. Ambartsumyan, O. Aimiwu, L. Richter, J. Zhang, et al. 2009. Induced pluripotent stem cells and embryonic stem cells are distinguished by gene expression signatures. *Cell Stem Cell.* 5:111–123. <https://doi.org/10.1016/j.stem.2009.06.008>
- Choi, J., S. Lee, W. Mallard, K. Clement, G.M. Tagliazucchi, H. Lim, I.Y. Choi, F. Ferrari, A.M. Tsankov, R. Pop, et al. 2015. A comparison of genetically matched cell lines reveals the equivalence of human iPSCs and ESCs. *Nat. Biotechnol.* 33:1173–1181. <https://doi.org/10.1038/nbt.3388>
- Deng, J., R. Shoemaker, B. Xie, A. Gore, E.M. LeProust, J. Antosiewicz-Bourget, D. Egli, N. Maherali, I.H. Park, J. Yu, et al. 2009. Targeted bisulfite sequencing reveals changes in DNA methylation associated with nuclear reprogramming. *Nat. Biotechnol.* 27:353–360. <https://doi.org/10.1038/nbt.1530>
- Desmarais, J.A., M.J. Hoffmann, G. Bingham, M.E. Gagou, M. Meuth, and P.W. Andrews. 2012. Human embryonic stem cells fail to activate CHK1 and commit to apoptosis in response to DNA replication stress. *Stem Cells.* 30:1385–1393. <https://doi.org/10.1002/stem.1117>
- Ding, Q., M.M. Edwards, M.L. Hulke, A.N. Bracci, Y. Hu, Y. Tong, X. Zhu, J. Hsiao, C.J. Charvet, S. Ghosh, R.E. Handsaker, K. Eggan, F.T. Merkle, J. Gerhardt, D. Egli, A.G. Clark, and A. Koren. 2020. The Genetic Architecture of DNA Replication Timing in Human Pluripotent Stem Cells. *bioRxiv:2020.2005.2008.085324.*
- Doi, A., I.H. Park, B. Wen, P. Murakami, M.J. Aryee, R. Irizarry, B. Herb, C. Ladd-Acosta, J. Rho, S. Loewer, et al. 2009. Differential methylation of tissue- and cancer-specific CpG island shores distinguishes human induced pluripotent stem cells, embryonic stem cells and fibroblasts. *Nat. Genet.* 41:1350–1353. <https://doi.org/10.1038/ng.471>
- Ge, X.Q., and J.J. Blow. 2010. Chk1 inhibits replication factory activation but allows dormant origin firing in existing factories. *J. Cell Biol.* 191:1285–1297. <https://doi.org/10.1083/jcb.201007074>
- Ge, X.Q., J. Han, E.C. Cheng, S. Yamaguchi, N. Shima, J.L. Thomas, and H. Lin. 2015. Embryonic Stem Cells License a High Level of Dormant Origins to Protect the Genome against Replication Stress. *Stem Cell Reports.* 5:185–194. <https://doi.org/10.1016/j.stemcr.2015.06.002>
- Gerhardt, J., M.J. Tomishima, N. Zaninovic, D. Colak, Z. Yan, Q. Zhan, Z. Rosenwaks, S.R. Jaffrey, and C.L. Schildkraut. 2014a. The DNA replication program is altered at the FMRI locus in fragile X embryonic stem cells. *Mol. Cell.* 53:19–31. <https://doi.org/10.1016/j.molcel.2013.10.029>
- Gerhardt, J., N. Zaninovic, Q. Zhan, A. Madireddy, S.L. Nolin, N. Ersalesi, Z. Yan, Z. Rosenwaks, and C.L. Schildkraut. 2014b. Cis-acting DNA sequence at a replication origin promotes repeat expansion to fragile X full mutation. *J. Cell Biol.* 206:599–607. <https://doi.org/10.1083/jcb.201404157>
- Gerhardt, J., A.D. Bhalla, J.S. Butler, J.W. Puckett, P.B. Dervan, Z. Rosenwaks, and M. Napierala. 2016. Stalled DNA Replication Forks at the Endogenous GAA Repeats Drive Repeat Expansion in Friedreich's Ataxia Cells. *Cell Rep.* 16:1218–1227. <https://doi.org/10.1016/j.celrep.2016.06.075>
- Guenther, M.G., G.M. Frampton, F. Soldner, D. Hockemeyer, M. Mitalipova, R. Jaenisch, and R.A. Young. 2010. Chromatin structure and gene expression programs of human embryonic and induced pluripotent stem cells. *Cell Stem Cell.* 7:249–257. <https://doi.org/10.1016/j.stem.2010.06.015>
- Hansel, M.C., R. Gramignoli, W. Blake, J. Davila, K. Skvorak, K. Dorko, V. Tahan, B.R. Lee, E. Tafaleng, J. Guzman-Lepe, et al. 2014. Increased reprogramming of human fetal hepatocytes compared with adult hepatocytes in feeder-free conditions. *Cell Transplant.* 23:27–38. <https://doi.org/10.3727/096368912X662453>
- Hiratani, I., T. Ryba, M. Itoh, J. Rathjen, M. Kulik, B. Papp, E. Fussner, D.P. Bazett-Jones, K. Plath, S. Dalton, et al. 2010. Genome-wide dynamics of replication timing revealed by in vitro models of mouse embryogenesis. *Genome Res.* 20:155–169. <https://doi.org/10.1101/gr.099796.109>
- Hyrien, O., C. Maric, and M. Méchali. 1995. Transition in specification of embryonic metazoan DNA replication origins. *Science.* 270:994–997. <https://doi.org/10.1126/science.270.5238.994>
- Johannesson, B., I. Sagi, A. Gore, D. Paull, M. Yamada, T. Golan-Lev, Z. Li, C. LeDuc, Y. Shen, S. Stern, et al. 2014. Comparable frequencies of coding mutations and loss of imprinting in human pluripotent cells derived by nuclear transfer and defined factors. *Cell Stem Cell.* 15:634–642. <https://doi.org/10.1016/j.stem.2014.10.002>
- Kappas, N.C., P. Savage, K.C. Chen, A.T. Walls, and J.C. Sible. 2000. Dissection of the XChk1 signaling pathway in *Xenopus laevis* embryos. *Mol. Biol. Cell.* 11:3101–3108. <https://doi.org/10.1091/mbc.11.9.3101>
- Kermi, C., E. Lo Furno, and D. Maiorano. 2017. Regulation of DNA Replication in Early Embryonic Cleavages. *Genes (Basel).* 8:42. <https://doi.org/10.3390/genes8010042>
- Kim, K., A. Doi, B. Wen, K. Ng, R. Zhao, P. Cahan, J. Kim, M.J. Aryee, H. Ji, L.I. Ehrlich, et al. 2010. Epigenetic memory in induced pluripotent stem cells. *Nature.* 467:285–290. <https://doi.org/10.1038/nature09342>
- Ku, S., E. Soragni, E. Campau, E.A. Thomas, G. Altun, L.C. Laurent, J.F. Loring, M. Napierala, and J.M. Gottesfeld. 2010. Friedreich's ataxia induced pluripotent stem cells model intergenerational GAA-TTC triplet repeat instability. *Cell Stem Cell.* 7:631–637. <https://doi.org/10.1016/j.stem.2010.09.014>
- Liang, G., and Y. Zhang. 2013. Genetic and epigenetic variations in iPSCs: potential causes and implications for application. *Cell Stem Cell.* 13:149–159. <https://doi.org/10.1016/j.stem.2013.07.001>
- Lister, R., M. Pelizzola, Y.S. Kida, R.D. Hawkins, J.R. Nery, G. Hon, J. Antosiewicz-Bourget, R. O'Malley, R. Castanon, S. Klugman, et al. 2011. Hotspots of aberrant epigenomic reprogramming in human induced pluripotent stem cells. *Nature.* 471:68–73. <https://doi.org/10.1038/nature09798>
- Maehr, R., S. Chen, M. Snitow, T. Ludwig, L. Yagasaki, R. Golland, R.L. Leibel, and D.A. Melton. 2009. Generation of pluripotent stem cells from patients with type 1 diabetes. *Proc. Natl. Acad. Sci. USA.* 106:15768–15773. <https://doi.org/10.1073/pnas.0906894106>
- Mandai, M., A. Watanabe, Y. Kurimoto, Y. Hirami, C. Morinaga, T. Daimon, M. Fujihara, H. Akimaru, N. Sakai, Y. Shibata, et al. 2017. Autologous Induced Stem-Cell-Derived Retinal Cells for Macular Degeneration. *N. Engl. J. Med.* 376:1038–1046. <https://doi.org/10.1056/NEJMoa1608368>
- Newman, A.M., and J.B. Cooper. 2010. Lab-specific gene expression signatures in pluripotent stem cells. *Cell Stem Cell.* 7:258–262. <https://doi.org/10.1016/j.stem.2010.06.016>
- Nishino, K., M. Toyoda, M. Yamazaki-Inoue, Y. Fukawatase, E. Chikazawa, H. Sakaguchi, H. Akutsu, and A. Umezawa. 2011. DNA methylation dynamics in human induced pluripotent stem cells over time. *PLoS Genet.* 7: e1002085. <https://doi.org/10.1371/journal.pgen.1002085>
- Norio, P., and C.L. Schildkraut. 2001. Visualization of DNA replication on individual Epstein-Barr virus episomes. *Science.* 294:2361–2364. <https://doi.org/10.1126/science.1064603>
- Park, I.H., P.H. Lerou, R. Zhao, H. Huo, and G.Q. Daley. 2008a. Generation of human-induced pluripotent stem cells. *Nat. Protoc.* 3:1180–1186. <https://doi.org/10.1038/nprot.2008.92>
- Park, I.H., R. Zhao, J.A. West, A. Yabuuchi, H. Huo, T.A. Ince, P.H. Lerou, M.W. Lensch, and G.Q. Daley. 2008b. Reprogramming of human somatic cells to pluripotency with defined factors. *Nature.* 451:141–146. <https://doi.org/10.1038/nature06534>

- Rajarajan, K., M.C. Engels, and S.M. Wu. 2012. Reprogramming of mouse, rat, pig, and human fibroblasts into iPS cells. *Curr Protoc Mol Biol.* Chapter 23:Unit-23 15.
- Ristow, M., H. Mulder, D. Pomplun, T.J. Schulz, K. Müller-Schmehl, A. Krause, M. Fex, H. Puccio, J. Müller, F. Isken, et al. 2003. Frataxin deficiency in pancreatic islets causes diabetes due to loss of beta cell mass. *J. Clin. Invest.* 112:527–534. <https://doi.org/10.1172/JCI18107>
- Ryba, T., I. Hiratani, J. Lu, M. Itoh, M. Kulik, J. Zhang, T.C. Schulz, A.J. Robins, S. Dalton, and D.M. Gilbert. 2010. Evolutionarily conserved replication timing profiles predict long-range chromatin interactions and distinguish closely related cell types. *Genome Res.* 20:761–770. <https://doi.org/10.1101/gr.099655.109>
- Ryba, T., I. Hiratani, T. Sasaki, D. Battaglia, M. Kulik, J. Zhang, S. Dalton, and D.M. Gilbert. 2011. Replication timing: a fingerprint for cell identity and pluripotency. *PLoS Comput. Biol.* 7. e1002225. <https://doi.org/10.1371/journal.pcbi.1002225>
- Santos, M.M., K. Ohshima, and M. Pandolfo. 2001. Frataxin deficiency enhances apoptosis in cells differentiating into neuroectoderm. *Hum. Mol. Genet.* 10:1935–1944. <https://doi.org/10.1093/hmg/10.18.1935>
- Schultz, S.S., S.C. Desbordes, Z. Du, S. Kosiyatrakul, I. Lipchina, L. Studer, and C.L. Schildkraut. 2010. Single-molecule analysis reveals changes in the DNA replication program for the POU5F1 locus upon human embryonic stem cell differentiation. *Mol. Cell. Biol.* 30:4521–4534. <https://doi.org/10.1128/MCB.00380-10>
- Schultz, M.D., Y. He, J.W. Whitaker, M. Hariharan, E.A. Mukamel, D. Leung, N. Rajagopal, J.R. Nery, M.A. Urich, H. Chen, et al. 2015. Human body epigenome maps reveal noncanonical DNA methylation variation. *Nature.* 523:212–216. <https://doi.org/10.1038/nature14465>
- Studer, L.. 2017. Strategies for bringing stem cell-derived dopamine neurons to the clinic-The NYSTEM trial. *Prog. Brain Res.* 230:191–212. <https://doi.org/10.1016/bs.pbr.2017.02.008>
- Sui, L., N. Danzl, S.R. Campbell, R. Viola, D. Williams, Y. Xing, Y. Wang, N. Phillips, G. Poffenberger, B. Johannesson, et al. 2018.  $\beta$ -Cell Replacement in Mice Using Human Type 1 Diabetes Nuclear Transfer Embryonic Stem Cells. *Diabetes.* 67:26–35. <https://doi.org/10.2337/db17-0120>
- Tachibana, M., P. Amato, M. Sparman, N.M. Gutierrez, R. Tippner-Hedges, H. Ma, E. Kang, A. Fulati, H.S. Lee, H. Sritanandomchai, et al. 2013. Human embryonic stem cells derived by somatic cell nuclear transfer. *Cell.* 153:1228–1238. <https://doi.org/10.1016/j.cell.2013.05.006>
- Takahashi, K., and S. Yamanaka. 2006. Induction of pluripotent stem cells from mouse embryonic and adult fibroblast cultures by defined factors. *Cell.* 126:663–676. <https://doi.org/10.1016/j.cell.2006.07.024>
- Takahashi, K., K. Tanabe, M. Ohnuki, M. Narita, T. Ichisaka, K. Tomoda, and S. Yamanaka. 2007. Induction of pluripotent stem cells from adult human fibroblasts by defined factors. *Cell.* 131:861–872. <https://doi.org/10.1016/j.cell.2007.11.019>
- van der Laan, S., N. Tsanov, C. Crozet, and D. Maiorano. 2013. High Dub3 expression in mouse ESCs couples the G1/S checkpoint to pluripotency. *Mol. Cell.* 52:366–379. <https://doi.org/10.1016/j.molcel.2013.10.003>
- Wakayama, S., T. Kohda, H. Obokata, M. Tokoro, C. Li, Y. Terashita, E. Mizutani, V.T. Nguyen, S. Kishigami, F. Ishino, et al. 2013. Successful serial recloning in the mouse over multiple generations. *Cell Stem Cell.* 12:293–297. <https://doi.org/10.1016/j.stem.2013.01.005>
- Wyles, S.P., E.B. Brandt, and T.J. Nelson. 2014. Stem cells: the pursuit of genomic stability. *Int. J. Mol. Sci.* 15:20948–20967. <https://doi.org/10.3390/ijms151120948>
- Yamada, M., B. Johannesson, I. Sagi, L.C. Burnett, D.H. Kort, R.W. Prosser, D. Paull, M.W. Nestor, M. Freeby, E. Greenberg, et al. 2014. Human oocytes reprogram adult somatic nuclei of a type 1 diabetic to diploid pluripotent stem cells. *Nature.* 510:533–536. <https://doi.org/10.1038/nature13287>

Supplemental material

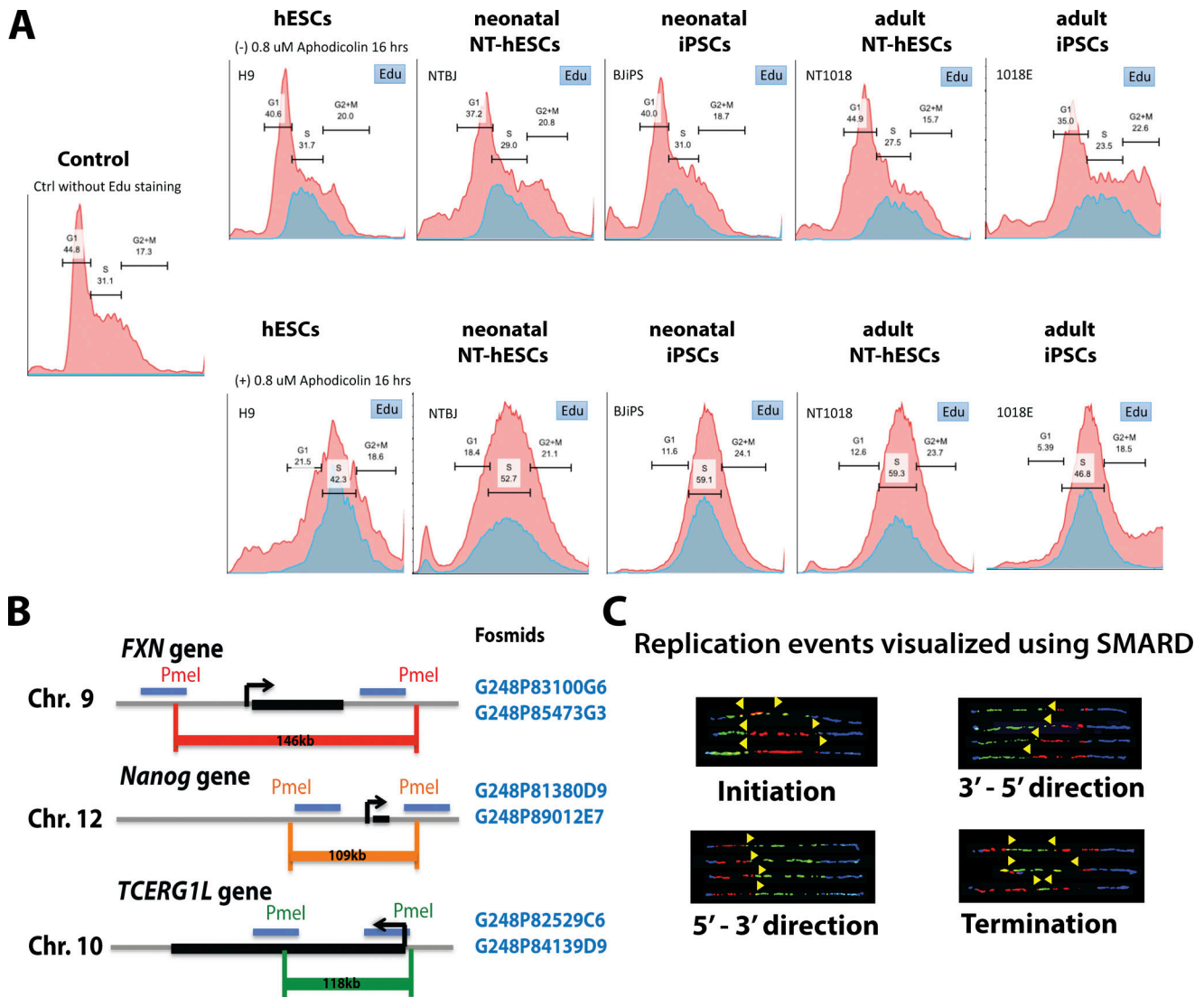


Figure S1. **Cell cycle analysis and SMARD.** Related to Figs. 1, 2, 3, 4, and 5. **(A and B)** Cell cycle analysis of PSCs and control (Ctrl). **(A)** Flow cytometry profiles of PSCs treated without (upper panel) and with aphidicolin (lower panel). Control (Ctrl) and PSCs profile are shown. **(B)** Map (location of chromosome, Chr.) of the genomic loci analyzed in this study; the *FXN* and *Nanog* gene loci are DNA segments where the DNA replication is regulated during cell development. The *TCERG1L* gene is a DMR. DMR loci contain abnormal DNA methylation in iPSCs. Genes are indicated in black and FISH probes in blue. Pmel fragments are shown in green, orange, and red. Fosmids used in SMARD experiments are indicated. **(C)** Detectable replication events using SMARD are shown.



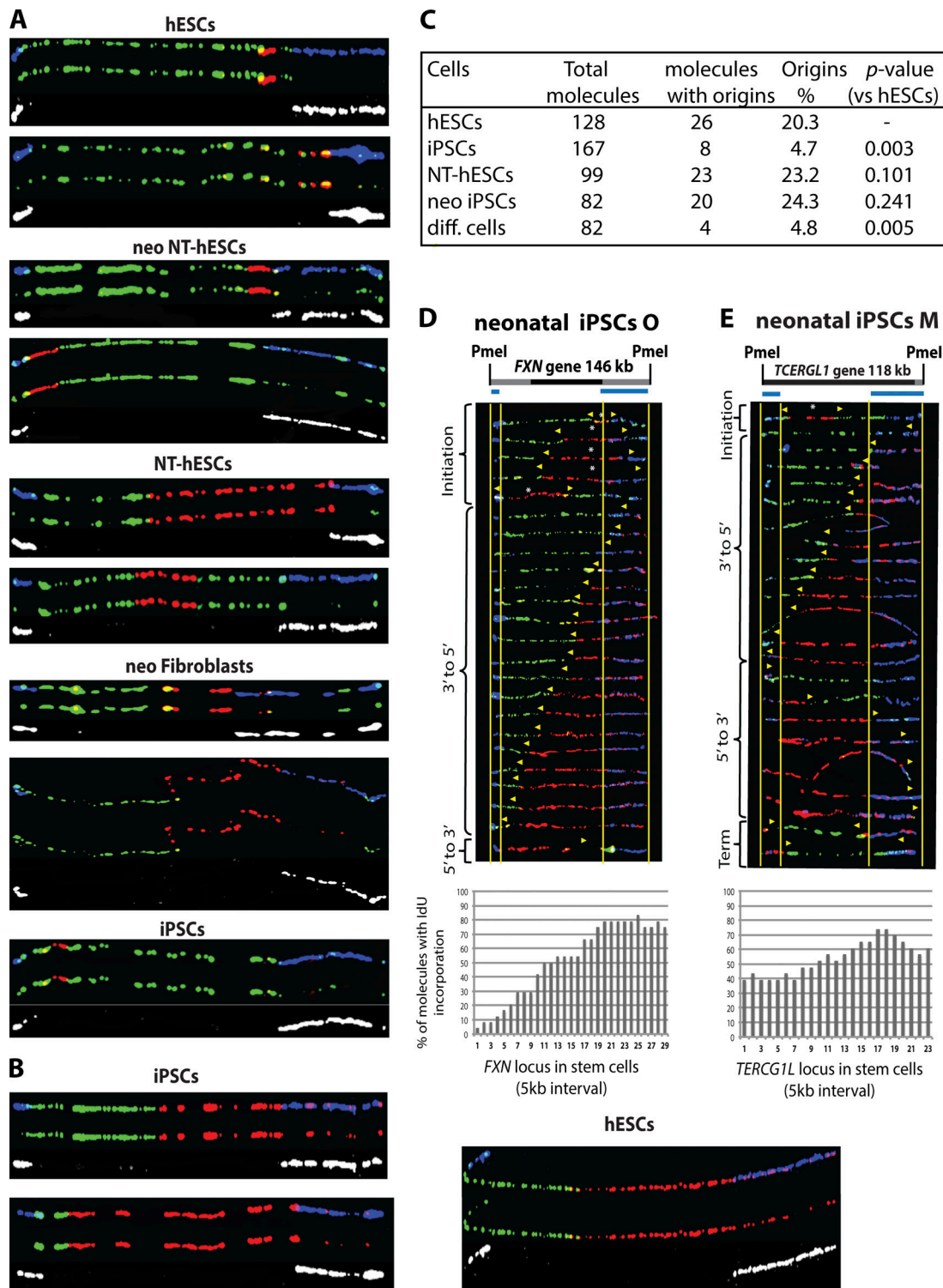
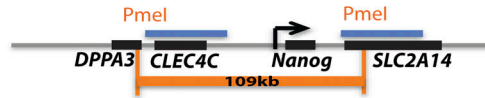
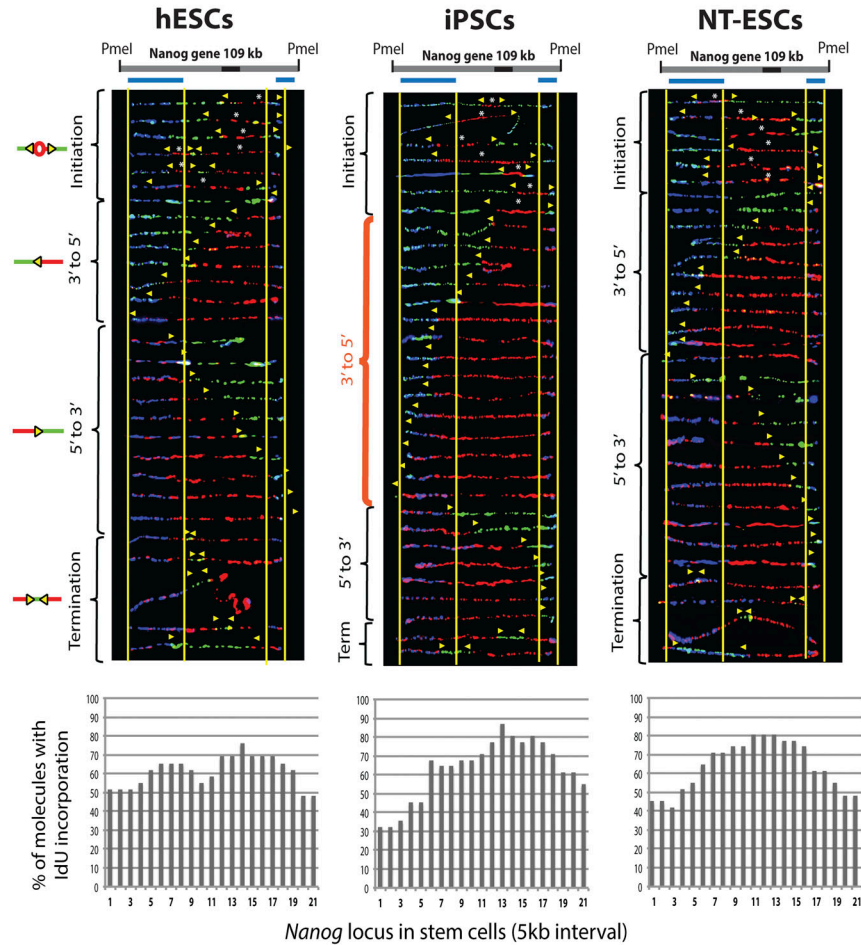


Figure S2. DNA replication program is not altered in a second neonatal iPSCs at the *FXN* and at the *TCERG1L* gene locus. Related to Figs. 2, 3, and 4. **(A and B)** Examples of SMARD molecules from each cell line are shown with higher resolution and separated by fluorescence colors. **(A)** Shown are molecules with replication origins. **(B)** Shown are molecules with replication forks in the 3' to 5' direction. **(C)** Table summarizing the total count of analyzed SMARD molecules at the *FXN* locus from three hESCs (WCMC4, Fig. 2 B; H9 and H14, Gerhardt et al., 2016), three iPSCs (iPSCs B and E, Fig. 3, A and B; and iPSCs NP, Gerhardt et al., 2016), two NT-hESCs (NT-hESCs, Fig. 2 D, and neonatal NT-hESCs, Fig. 2 E), two neonatal (neo) iPSCs (Fig. 3, C and D), and two diff. cells (neonatal fibroblasts, Fig. 2 C; and diff. H9 cells, Gerhardt et al., 2016; standard deviation and P values are indicated in the diagram) and percentage of the molecules containing a replication origin per each cell line. **(D and E)** Top: Map of the PmeI segment containing the *FXN* gene or *TCERG1L* gene. The positions of the FISH probes are marked in blue. Middle: Photomicrographs of labeled DNA molecules from neonatal (neo) iPSCs M (D) and neonatal iPSCs (E) are ordered according to replication fork (yellow arrows) progression in the 5'-3' and 3'-5' directions; replication initiation; and termination. Bottom: The percentage of molecules with IdU incorporation (first pulse) is calculated from the DNA molecules shown above.

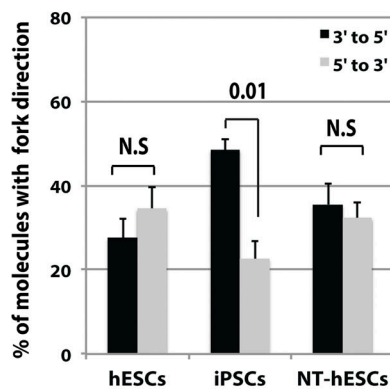
**A** *Nanog* gene locus



**B**



**C**



**D**

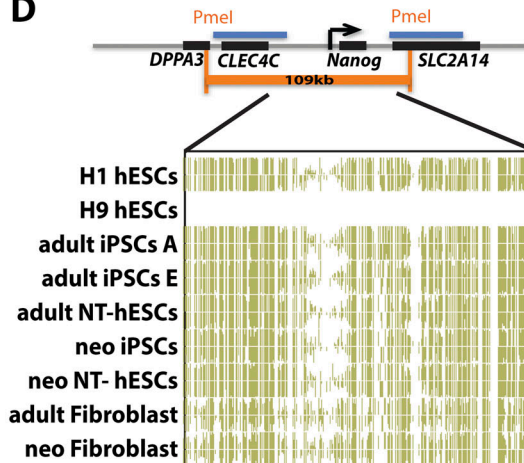


Figure S3. **DNA replication is altered at the developmentally regulated *Nanog* gene locus in iPSCs compared with hESCs.** Related to Fig. 2. **(A)** Map of the *Nanog* segment with adjacent genes and DNA segment analyzed by SMARD (orange). **(B)** Top: Map of the *Nanog* segment with FISH probes. Middle: Photomicrographs of labeled DNA molecules from hESCs, iPSCs, and NT-hESCs are ordered according to replication fork (yellow arrows) progression in the 5'-3' and 3'-5' directions; replication initiation; and termination. Bottom: The percentage of molecules with IdU incorporation (first pulse) in hESCs, iPSCs, and NT-hESCs is calculated from the DNA molecules shown above. **(C)** Diagram of the percentage of DNA molecules with replication fork in 3'-5' and 5'-3' direction in hESCs, iPSCs, and NT-hESCs. Standard deviation and P values are indicated in the diagram (P values hESCs = 0.2 and NT-hESCs 0.48). **(D)** CpG methylation analysis of the *Nanog* gene locus using bisulfite sequencing (methylation in H9 cells was not analyzed at this locus).

Cells	Average(%) Replication Forks 5 kb DNA segment	Standard deviation	Range Lowest-Highest % of Replication forks/ 5 kb DNA segment
hESCs	4.275	1.750	0 - 6.00
hESCs+Aphidicolin	4.083	3.032	0 - 7.89
iPSCs	3.523	2.811	0 - 8.69
iPSCs+Aphidicolin	4.868	4.465	0 - 14.70
NT-hESCs	4.525	3.053	0 - 10.4
NT-hESCs+Aphidicolin	4.138	2.709	0 - 8.57

Figure S4. **Replication fork progression is altered in adult iPSCs compared with hESCs.** Related to Fig. 5. Table summarizes the average percentage of molecules containing a replication fork per each 5-kb DNA interval over the entire 146-kb PmeI fragment of the *FXN* gene locus in hESCs, adult iPSCs, and NT-hESCs (Fig. 5, E-G). Standard deviation and the lowest and highest percentage of forks per each 5-kb segment for each cell lines are indicated.

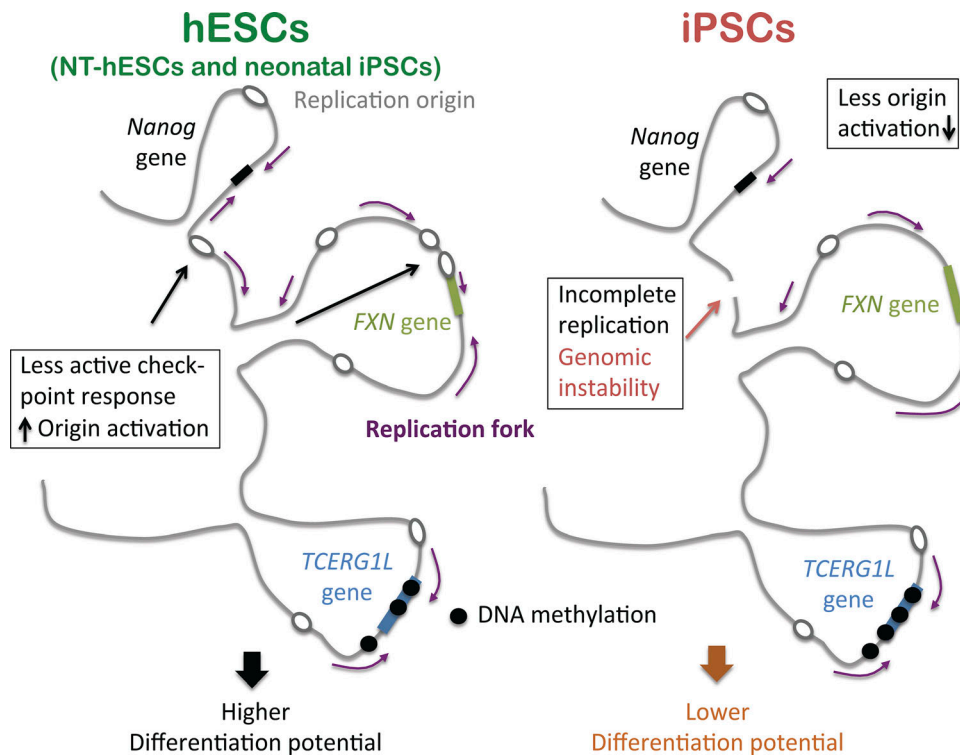


Figure S5. **Model for replication defects in PSCs that lead to genomic instability and altered cell differentiation potential.** Related to Figs. 1, 2, 3, 4, and 5. ESCs have been shown to have a higher density of replication origins, which has been suggested to be an important factor for sufficient cell growth and genomic stability at early developmental stages. In addition, it has been shown that ESCs have more replication origins than adult cells because of a less rigid checkpoint response. Our data show fewer replication initiation sites in iPSCs, which seems to be the result of an altered response to aphidicolin. A decrease in replication initiation sites could impede the completion of DNA synthesis in these cells, causing genomic instability and lowering the differentiation potential of PSCs. However, reprogrammed NT-hESCs and neonatal iPSCs with a similar number of replication origins as hESCs are less prone to genomic instabilities.